The techno-economics of biocarbon production processes under Norwegian conditions

Maciej Olszewski[a,c], Rajesh S. Kempegowda[b], Øyvind Skreiberg[b], Liang Wang[b], Terese Løvås[a]

[a]Department of Energy & Process Engineering, NTNU, Trondheim, Norway

[b]SINTEF Energy Research, Trondheim, Norway

[c]AGH University of Science and Technology, Faculty of Energy and Fuels, Krakow, Poland

Corresponding author: rajesh.kempegowda@sintef.no

Abstract

This work deals with techno-economic analysis studies in the context of production of various grade biocarbon for utilization as reducing agents in metallurgical industries. A detailed process design was developed for wood handling, debarking, chipping, drying, carbonization, and combined heat and power production using Aspen Plus for 10 ton per day (TPD) biocarbon output. A Fortran based user defined function was developed for the carbonization process by considering pressure, temperature and particle size effects using a Box – Behnken approach. The empirical correlation indicates a strong influence of temperature as well as a significant influence of pressure and particle size on the biocarbon yield and its fixed carbon content. Fixed carbon content increases with temperature, pressure and particle size. Mass and energy balance results from Aspen Plus provided necessary results for cost parametrization considering three influencing parameters; temperature, pressure and plant scale on the equipment costs, operating expenses and production cost of biocarbon. Four scenarios are compared i.e. logwood supply, woodchips supply, co-production of biooil and replacing the carbonization agent from nitrogen to air. The results indicate that logwood supply is more economical than supplying woodchips to the plant gate. Economic benefits in terms of cost is ~5% (at 1 bar and 450-500ºC, 55-60 TPD) and ~4% (at 10 bar, 450-500ºC, 55-60 TPD). Co-production of biooil decreased the production cost of biocarbon ($/GJ) by 40-44% (at 1 bar, 450-500ºC, 40-60 TPD) and 30-36% (at 10 bar, 450-500ºC, 40-60 TPD), respectively. Finally, the economic return based on IRR suggests that highest IRR is achieved for scenario C, where biooil is a co-product, it is due

This is the post-print version.
Published version dx.doi.org/10.1021/acs.energyfuels.6b03441

to high market price of woody tar at 500 $/ton. Transportation of forest biomass (logwood) from 20 to 220 km increased the cost of logwood from 4.75 $/GJ to 7.15 $/GJ, which is significant in terms of operating cost.

Keywords: Biocarbon/Charcoal, Carbonization, Process design and simulation, parametric cost modelling

1. Introduction

Norwegian metal production industries are facing challenges with respect to CO_2 emissions. According to Statistics Norway [1], metallurgical industries use large quantities of pit coal briquettes, about 541990 tons per year, and coal coke and semi-coke, around 353818 tons per year, as reducing agent during production. As well, wood charcoal is used in these sectors in the amount of 26000 tons annually. Under Norwegian conditions, 100% of the charcoal is imported. The major source of bioenergy in Norway is forest biomass [2] and the main kinds of trees are spruce, pine, birch and alder [3]. In that perspective, Norway has potential to utilize forest woody biomass as an attractive alternative feedstock for the production of high value energy carriers such as charcoal/biocarbon. Charcoal/biocarbon is produced in a thermochemical conversion process that operates under inert atmosphere or starved oxygen condition called carbonization [4, 5]. Traditional carbonization processes are heavily criticized due to the low yield of charcoal and direct emissions generated by these industries [6]. Charcoal is considered to be an international commodity; charcoal production in these traditional production processes demands a long residence time and gives a low charcoal yield [4, 7]. According to worldwide charcoal utilization, 50 million tons of charcoal is consumed for various industrial uses, for example as reducing agent [8], co-firing and as a domestic cooking fuel in developing countries [6]. With an assumption of 15% average charcoal yield on dry wood basis, there is a consumption of 1 billion m^3 of woody biomass. Hence, there is a demand for more sustainable charcoal production processes to be applied in the industrial sector. As well in the European region, there is large consumption of coal, coke and other fossil derived synthetic carbon as reductants in the metal production industries. This is causing a wide range of damaging effects such as emission intensity raise and health hazards. To tackle the low yield charcoal production processes and improve the economic viability, self-sustainable production of charcoal under Norwegian conditions is highly relevant. Carbonization processes can be classified based on the temperature regimes of operation in the pyrolysis process as a low temperature carbonization (torrefaction) and high temperature carbonization. This depends on the use of upgraded biomass of different grades for the purpose of reducing agent in metal production furnaces or co-firing in furnaces or boilers. Biocarbon product quality is normally assessed based on the fixed carbon content as the main quality index criteria in several metallurgical industries. Aluminum production requires very high fixed carbon content, above 95%, whereas SiMn and FeMn around 95%, Si and FeSi above 70% and SiC above 80%. In that perspective, carbonization process operating conditions, as peak temperature in the carbonization process, have an influential effect on reaction paths and biocarbon properties [9, 10]. However increasing the temperature reduces the yield of charcoal. This demands a process that can mimic the natural process occurring under the earth based on an elevated pressure, which plays a significant role in improving the yield of charcoal and fixed carbon. Studies on the influence of elevated pressure dates back to 1853, started by Violette et al. [11]. Later, there is decades of experience from University of Hawaii, and also in collaboration with Norwegian researchers, by Antal and coworkers on the influence of elevated pressure in a flash type carbonization reactor for various feedstocks [9, 12-14]. Recently, a few works from Australia in the area of improved charcoal production using an auto-thermal reactor at atmospheric

This is the post-print version.
Published version dx.doi.org/10.1021/acs.energyfuels.6b03441

conditions have been reported [15, 16]. Other important parameters that govern the process are vapor residence time and heating rates, influencing the charcoal yield and fixed carbon content [9, 17]. Depending on the process operating conditions and process reactor the quality of biocarbon in terms of fixed carbon content, reactivity, porosity and surface area will be influenced. Based on these properties, biocarbon can be utilized for cooking, residential heating, peak load boilers, adsorbent, soil conditioning and metallurgical production. In this context, a detailed techno-economic evaluation of carbonization processes based on plant-gate analysis is carried out under Norwegian conditions. This work deals with techno-economic studies in the context of production of various grade biocarbon as reducing agents and for co-firing in the metallurgical industries. The plant gate analysis involves process system analysis using Aspen Plus with user defined functions development using Fortran expressions for the wood handling zone consisting of debarking, chipping, drying, carbonization process and combined heat and power (CHP) production. This study also investigates the influence of process conditions such as carbonization temperature, pressure and particle size on the overall biocarbon yield through semi-empirical methods. The case design is developed based on the principles of an integrated process system analysis approach. A novel simplified multifunctional regression model has been proposed to predict the product yields as a function of the carbonization process parameters temperature, pressure and particle size. The study also integrates a heat and power system coupled to the carbonization process to produce electricity and provide heat to external customers, e.g. district heat production. A techno-economic value chain is designed for the supply of biomass from the Norwegian forest, for example spruce, as a potential feedstock.

2. Process plant design and approach

This is the post-print version.
Published version dx.doi.org/10.1021/acs.energyfuels.6b03441

Figure 1 shows the process flow diagram for the biomass carbonization plant. Main process steps are i) feedstock handling consisting of stem wood storage, debarking, chipping and screening, chips drying, ii) carbonization process and iii) combined heat and power production. Process plant design is carried out in the commercial software Aspen Plus using user defined Fortran programming. The commercial process simulation software is based on the basic engineering relations (mass and energy balance, phase equilibrium and reaction kinetics). This allows simulating process behaviors including chemical reactions. It is possible to simulate one block element or the complete integrated system for different process configurations. In this work, the Peng – Robinson equation of state was used for properties determination. The advantage of using a cubic form is that it has capability to handle non ideal behavior for hydrocarbons [18]. Details of the process models developed in each process zone are presented below.

2.1 Feedstocks characteristics

Norwegian spruce biomass is considered as the feedstock. Fuel characterization such as proximate analysis, ultimate analysis and heating values are shown in Table 1 for spruce stem wood, spruce woodchips, spruce bark and spruce forest residues.

2.2 Process modelling and simulation

Logwood handling system modelling in Aspen Plus: Logwood harvested from the forestry is transported via trucks to the carbonization plant. Logwood harvested will have a cut length of 3 m. The diameter of the logwood can vary from 0.15 m to 0.5 m (Norwegian Institute of Bioeconomy Research). Logwood handling system consists of debarking to remove the bark, chipping, screening and drying as shown in Figure 2. Details of the sub-process models are depicted in the following subsections.

This is the post-print version.
Published version dx.doi.org/10.1021/acs.energyfuels.6b03441

Debarking process: Traditionally, bark separation from the stem wood was usually carried out for pulping processes. The advantage of bark separation in the pulping process is to reduce the cooking chemical consumption as well as to avoid contamination due to ash rich compounds (silica and calcium compounds, dirt) [19]. Similarly, bark separation is also relevant in the biocarbon production for metallurgical industry. The amount of bark on the stem wood varies according to tree species, for spruce 8-15%, for birch 7-15% and for pine 10-17% [20]. According to standard EN14961-2, production of Class A1 pellets from bark for energy purpose is not suitable due to the high ash content in the bark. In a drum debarker, the volumetric loading is in the range of 25-35% with a drum speed around 4-7 rpm. In our estimation we used industrial data (length: 18 m and 5 m diameter) and a residence time in the debarking process of around 40 mins (Jan 2016). In the Aspen Plus system model, a simple splitter model is used with user defined expressions. Specific electricity consumption P [kW] for the debarker (DE) was calculated as shown in equation 1, where X_{DE} – electricity consumption for static load [kW], S_{DE} – static load [kg/h] and M_{LOG} – logwood mass flow rate [kg/h]. In the model power requirement for debarker (X_{DE}) is 34.5 kW and the static load (S_{DE}) is 85000 kg/h.

$$P_{DE} = \frac{X_{DE}}{S_{DE}} \cdot M_{LOG} \qquad (1)$$

This is the post-print version.
Published version dx.doi.org/10.1021/acs.energyfuels.6b03441

Chipping and screening: Quality specifications and classes selected in the biocarbon process value chain is based on the European standards (e.g. EN 14961-1), this includes all solid biofuels and it is probably targeted for industries, even though it is meant for all groups. The particle sizes are classified according to standard EN 15149-1. Typically, metallurgical industries require an ash content below 3% [21]. The chipper model is based on industrial scale data, implemented as a Fortran expression in the model. Specific power consumption P [kW] for the chipper (CH) is based on mass flow rate into the chipper according to equation 2.

$$P_{CH} = \frac{X_{CH}}{S_{CH}} \cdot M_{IN-CHIP} \qquad (2)$$

where X_{CH} – electricity consumption for static load [kW], S_{CH} – static load [kg/h] and $M_{IN-CHIP}$ – mass flow rate into the chipper [kg/h]. A power consumption X_{CH} of 522.5 kW and a corresponding static load S_{CH} of 36000 kg/h are used as a model parameters. The screening model is based on the Aspen Plus built in model. Weight fractions data are gathered from Laitila et al. [22]. Weight fractions for the drum and disc chipper used in the model are shown in Table 2.

Chips drying: The belt dryer model use air as a drying medium. Heat is supplied by flue gas and LP steam from the CHP unit. Drying rate is calculated based on a drying curve for woodchips, experimental data is gathered from Johansson et al. [23], and the normalized drying rate $v(\alpha)$ according to equation 3 is implemented in Aspen Plus, and are shown in Figure 3 and also included as supplementary data in Appendix D.

$$v(\alpha) = \frac{\text{current drying rate}}{\text{drying rate 1st drying period}} \qquad \alpha = \frac{Z - Z_{eq}}{Z_{cr} - Z_{eq}} \qquad (3)$$

where α – normalized moisture content, Z – current moisture content on dry basis [kg/kg], Z_{cr} – Critical moisture content on dry basis (0.831 kg/kg), Z_{eq} – equilibrium moisture content on dry basis (0.01 kg/kg)[24] depends on the relative humidity and temperature of the drying medium, air. The drying rate is expressed in kg/(kg/s). For our drying conditions, reaching a moisture content of 10% is a reasonable assumption, and the normalised drying

This is the post-print version.
Published version dx.doi.org/10.1021/acs.energyfuels.6b03441

rate have in this work been applied until achieving this moisture content. Air goes first through heat exchangers (HE) where heat from the recycled air is recovered, next the air is preheated by flue gas, and the last heat exchanger is used when flue gas is not sufficient to provide all the heat needed and then low-pressure steam is used. Hot air is split into two streams, that are directed to the second and third stages. After that they are mixed and directed to the first stage as shown in Figure 4. The heat demand is dependent on the moisture content in the feedstock.

Carbonization process modelling: A schematic is shown in Figure 5. The heart of the process design is the carbonization reactor. The sub-model for the carbonization reactor is modelled through development of an empirical multifunctional regression model using experimental yields from several literature sources [4, 9, 10, 25]. The yields data are included as supplementary data in Appendix C. The model for the carbonization/pyrolysis is based on an user defined yield calculator using Fortran expressions. Heat to the reactor is supplied by flue gas. The pressure in the pressurized pyrolysis is provided by compressed nitrogen or air, where the air in this work is considered inert with respect to the pyrolysis products prediction. Pyrogas and biooil are burnt in the combustor to produce heat for the pyrolysis process and for CHP production. The main product is biocarbon.

<u>Pyrolysis modeling to predict products:</u>

This is the post-print version.
Published version dx.doi.org/10.1021/acs.energyfuels.6b03441

Pyrolysis modeling to predict products is done in accordance with Neves et al. [26]. The model allows prediction of the carbon, hydrogen and oxygen (CHO) composition of produced biocarbon [kg/kg dry ash free biocarbon] based on empirical equations, which are correlated to temperature (T) in °C:

$$Y_{C,BC} = 0.93 - 0.92 \cdot \exp(-0.42 \cdot 10^{-2} \cdot T) \text{ , } R^2 = 0.65 \quad (4)$$

$$Y_{H,BC} = -0.41 \cdot 10^{-2} + 0.10 \cdot \exp(-0.24 \cdot 10^{-2} \cdot T) \text{ , } R^2 = 0.75 \quad (5)$$

$$Y_{O,BC} = 0.07 + 0.85 \cdot \exp(-0.48 \cdot 10^{-2} \cdot T) \text{ , } R^2 = 0.56 \quad (6)$$

These equations are reasonable and validated for woody biomass by Neves et al. [26]. Woodchips produced in the chipper below 3.15 mm becomes dust (sawdust) and above 45 mm is reintroduced into the chipper. The model was developed by gathering literature data for the biocarbon yield.

Biocarbon yield by statistical design:

Biocarbon yield ($Y_{biocarbon}$) was introduced by a Box – Behnken approach. This approach is rotatable and requires three levels for each factor. The main purpose is to optimize the response surface, which is impacted by the process condition [27, 28]. This approach can be expressed by equation 7.

$$y = \beta_0 + \sum_{i=1}^{k} \beta_i x_i + \sum_{i=1}^{k} \beta_{ii} x_i^2 + \sum_{i=1}^{k-1} \sum_{j=2}^{k} \beta_{ij} x_i x_j + \varepsilon \quad (7)$$

where $x_1, x_2, \ldots, x_k$ are the input variables which influence the response of y, β_0, β_i, β_{ii} ($i = 1, 2, \ldots, k$), β_{ij} ($i = 1, 2, \ldots, k$; $j = 1, 2, \ldots, k$) are unknown parameters and ε is a random error. The β coefficients are obtained by the least squares method [27]. The developed biocarbon yield [kg/kg dry biomass] function ($Y_{biocarbon}$) is shown in equation 8.

$$Y_{biocarbon} = 126.3 - 0.3406 \cdot T - 4.5 \cdot p + 4.13 \cdot d + 0.00031 \cdot T^2 + 0.19 \cdot p^2 - 0.204 \cdot d^2 \quad (8)$$

$$+ 0.0050 \cdot T \cdot p - 0.00971 \cdot T \cdot d + 2.29 \cdot p \cdot d, \quad R^2 = 0.90$$

where T is temperature in °C, p is pressure in bar and d is particle diameter in mm.

Published version dx.doi.org/10.1021/acs.energyfuels.6b03441

Gas yields [kg/kg dry ash free biomass] are based on empirical equations which are functions of temperature (T in °C, in the range 350 – 1000 °C) [26]. Main gas compounds in the pyrolysis gas are usually H_2O, H_2, CH_4, C_2H_4, CO and CO_2.

$$\mathrm{Y_{H2}} = 1.145 \cdot (1 - \exp(-0.11 \cdot 10^{-2} \cdot \mathrm{T}))^{9.384}, \quad R^2 = 0.94 \qquad (9)$$

$$Y_{CO} = Y_{H2} \cdot \frac{1}{3 \cdot 10^{-4} + \frac{0.0429}{1 + (T/632)^{-7.23}}}, \quad R^2 = 0.73 \qquad (10)$$

$$Y_{CH4} = -2.18 \cdot 10^{-4} + 0.146 \cdot Y_{CO}, \quad R^2 = 0.88 \qquad (11)$$

Additionally an equation for the pyrolysis gas LHV in MJ/kg was used to calculate the energy balance of the pyrolysis process (T in °C) [26].

$$LHVgas = -6.23 + 2.47 \cdot 10^{-2} \cdot T, \quad R^2 = 0.78, \ 300\text{-}900°C \qquad (12)$$

The Neves et al. [26] correlations indicate that there is a weak relationship between the elemental composition of tar and pyrolysis temperature. The recommended correlations [26] for the tar elemental composition [kg/kg dry tar] is shown in equations 13 to 15.

$$\mathrm{Y_{C,tar}} = 1.14 \cdot \mathrm{Y_{C,biomass}} \qquad (13)$$

$$\mathrm{Y_{H,tar}} = 1.13 \cdot \mathrm{Y_{H,biomass}} \qquad (14)$$

$$\mathrm{Y_{O,tar}} = 0.80 \cdot \mathrm{Y_{O,biomass}} \qquad (15)$$

where $Y_{i,biomass}$ is the biomass elemental composition [kg/kg, dry ash free basis].

The products carbon dioxide (CO_2), ethylene (C_2H_4) and biooil (organics and water) are calculated based on (C, H, O) balances and energy balance based on LHV by solving a set of equations in the spreadsheet solver. The reader should understand that by implementing this pyrolysis products modelling approach the pressure influence only adheres directly to the biocarbon yield and indirectly to the yields of biooil and gas, however, not directly to their composition. I.e. this means that to satisfy conservation of mass, elements and energy, the unknowns in the gas composition must be adjusted accordingly. As C_2H_4 is a minor species compared to the other remaining unknown carbon containing gas species, i.e. CO_2, the CO_2 concentration must then be adjusted to satisfy the conservation laws. Even if this

This is the post-print version.
Published version dx.doi.org/10.1021/acs.energyfuels.6b03441

results in an incorrect gas composition as a function of pressure, this do not really matter in this work, as it is the energy content and the elemental composition of the gas that matters, and not the species composition.

The model assumes that biooil consists of two model compounds, acetic acid (CH_3COOH) and phenol (C_6H_6O), in addition to water. The mass ratio is assumed to be 1:1 when closing the mass balance, which is reasonable assumption due to decomposition of cellulose and lignin in a wider temperature range for slow pyrolysis conditions. The yield functions developed in the Excel solver are reintroduced as Fortran functions in Aspen Plus. The model is able to close both mass and energy balances in the temperature range of 300 to 500°C and in the pressure range 1-20 bar. Mass balance results for the carbonization model at 500°C and varied pressure are shown in Table 3. According to the validated results, the gas yields do not change very significantly for pressurized carbonization under slow pyrolysis conditions [29].

Pyrolysis reactor sizing and scaling:

The concept of the pressurized reactor is based on Flash Carbonization™ by Antal et al. [12, 29, 30]. The design idea is to use 2 or 3 pressurized vessels in a swing mode (semi – continuous) as shown in Figure 6(a) and (b). Woody biomass dried in the belt drier is conveyed to the pyrolysis reactor and pressurized to the desired carbonization pressure by the carbonization agent, nitrogen or air. Nitrogen to carbonization reactor is used based on the experimental data of Lucas et al. [4]. The heat for the carbonization process is supplied by flue gas. As a simplification in this work, the pyrolysis products modelling is independent of using nitrogen or air as carrier gas, i.e. they are both considered inert agents. This is a justifiable assumption as in the case of air the amount used is too low to support gasification of char, and hence a direct influence of the air addition on the pyrolysis process and its products yield can be neglected. This assumption then enables using the same biocarbon yield model independent of the carrier gas, and the choice of the Flash Carbonization reactor then becomes a generic choice.

CHP: The Aspen CHP flow sheet is presented in Figure 7. Pyrolysis volatiles (biooil) and non-condensable gases are combusted in the combustor. The combustor is simulated by the built-in Aspen Plus Gibbs reactor model. Hot flue gas is passing through a series of heat exchangers (superheater, re-heater, evaporator and flash drum using built in Aspen Plus heat exchanger models). This mimics an industrial boiler [31], and remaining heat from the flue gas is passing through the economizer and air preheater. The flue gas after the air preheater supplies heat to the dryer. Part of the flue gas after the superheater is used to supply heat to the pyrolysis reactor (as shown in Figure 7). After heat recovery the flue gas goes to the stack. The production of steam is fixed to 700 kg/h independently from operating conditions, because the amounts and quality of pyrolysis gas and biooil is varying. HP steam is produced with a steam quality of 550 °C and 60 bar, and the power to steam ratio is kept constant at 0.18. HP steam is expanded in a series of steam turbines (high pressure, intermediate pressure and low pressure) where electricity is produced. LP steam after the LP turbine is used for drying and district heat production. Recycled condensed steam is mixed with the make-up water and pumped to the economizer.

Details of the design specifications implemented in Aspen Plus are shown in Table 4. The pressure was limited to 10 bar to avoid extreme combinations of parameters according to the Box – Behnken approach.

3. Biocarbon process system efficiency analysis

The details of the mass and energy flows for major identified streams are supplemented as respectively appendixes A and B for the 10 TPD biocarbon output base case plant. The tables includes the effect of carbonization process conditions (T, P) on the mass and energy flows through the system for logwood entering the plant with 40% moisture content on wet basis, which is according to the PFD shown in Figure 1. Based on the mass and energy flows simulation results, overall system efficiencies, that is biocarbon energy efficiency, district heat (hot water) efficiency, electricity generation efficiency and overall heat utilization efficiency are illustrated below. The mass and energy flows are also used in the techno-economic analysis.

3.1 Biocarbon energy efficiency

Elevated pressure results in increased biocarbon yield and higher fixed carbon yield as shown in Figure 8(a) and (b), where the fixed carbon yield [kg/kg dry ash free biomass] is defined by

$$y_{fC} = Y_{biocarbon} \cdot \frac{FC}{100 - A} \qquad (16)$$

where FC – percent fixed carbon content in the dry biocarbon on mass basis, A – percent ash content in the dry biomass on mass basis and the biocarbon yield [kg/kg dry biomass], is defined as

$$Y_{biocarbon} = \frac{m_{biocarbon}}{m_{biomass}} \qquad (17)$$

where $m_{biocarbon}$ is the mass flow rate of dry biocarbon [kg/h] and $m_{biomass}$ is the mass flow rate of dry biomass [kg/h].

As well, to utilize biocarbon in metal production industries, quality criteria for the biocarbon product vary depending on the type of metal production industry, but generally the fixed carbon content should be above 70%. This means increasing the operating temperature to 400 – 500 °C. The feedstock moisture content does not influence the biocarbon energy efficiency, since in each case the feedstock is dried to 10% moisture content on wet basis before entering the carbonization reactor, however, it influences on the additional energy requirement for heating up the moisture/water vapor in the pyrolysis process. Hence, in this work we have not studied the effect of moisture content on the carbonization process. Even though the moisture content in the feedstock may have an influence on the biocarbon yield, we have kept the moisture content of 10% on wet basis which is a reasonable assumption based on the experimental results from Antal et al. [7]. However, increased pressure gives an increased biocarbon yield while both increasing pressure and temperature also give an increased fixed carbon yield. This means that there is a coupling between pressure and temperature in increasing the fixed carbon yield, which is also confirmed by the literature [4, 9, 13]. In this model the fixed carbon content is only dependent on temperature.

Biocarbon energy efficiency is defined as

$$\eta_{\mathrm{biocarbon}} = \frac{m_{\mathrm{biocarbon}} \cdot \mathrm{HHV}_{\mathrm{biocarbon}}}{m_{\mathrm{biomass}} \cdot \mathrm{HHV}_{\mathrm{biomass}}} \qquad (18)$$

where, m – mass flow rate [kg/h], HHV – higher heating value [MJ/kg]. Effect of operating pressure and temperature on the biocarbon energy efficiency is shown in Figure 8(c). The trend shows that biocarbon energy efficiency decreases as the peak temperature increases from 300-500 °C, because of volatiles losses (Figure 8(a)). However, these volatiles losses favors an increased fixed carbon content in the biocarbon (Figure 8(b)).

3.2 Effect of feedstock moisture content on district heat efficiency

District heat efficiency is defined as

$$\eta_{\mathrm{DH}} = \frac{Q_{\mathrm{DH}}}{m_{\mathrm{biomass}} \cdot \mathrm{HHV}_{\mathrm{biomass}}} \qquad (19)$$

where Q_{DH} – heat available for district heat production [MJ/h]. Moisture content has strong influence on district heat efficiency (Figure 9). Increasing the pyrolysis temperature improves district heat efficiency (Figure 9), which is because the production of volatiles are higher and they are used as fuel. Increasing the pressure causes a slight decrease in district heat efficiency because it favors secondary pyrolysis reactions and hence less tar is produced. For the wood having 60% moisture, there is no district heat production for export,

This is the post-print version.
Published version dx.doi.org/10.1021/acs.energyfuels.6b03441

all the low-pressure steam is consumed for thermal drying of the feedstock (Figure 9(c)). Extra heat is needed and this penalty equals 8 – 9.4% of the HHV of input biomass.

3.3 Electricity generation efficiency

Electricity generation efficiency is defined as

$$\eta_{el} = \frac{3.6 \cdot P_{el}}{m_{biomass} \cdot HHV_{biomass}} \qquad (20)$$

where P_{el} – electricity output from the turbines [kW]. Base case steam production is fixed to 700 kg/h at all operating conditions. This is due to variations in the quality and quantity of produced fuel (pyrolysis gas and biooil). At lower temperatures less fuel is produced and 700 kg/h is minimum steam load. Base case electricity produced in the steam turbine is 127.95 kW, which is according to the fixed steam load to the turbine. Total production of biocarbon is set to 10 TPD biocarbon output in the base case model. Raw feedstock mass flow rate is changing according to biocarbon yield, which is a function of temperature and pressure. Electricity consumption is calculated based on mass flow rate in each equipment. Electricity generation efficiency is shown in Figure 9(d). Electricity generation efficiency decreases with increasing temperature, which is because the yield of biocarbon decreases. However, the steam load is set to minimum level and a portion of the steam is fed to the drying zone, which is depending on the moisture content. Low-pressure steam bleeded from the steam turbine is used for the district heat production.

3.4 Effect of feedstock moisture content on overall heat utilization efficiency

Overall heat utilization efficiency is defined as

$$\eta_{overall} = \eta_{biocarbon} + \eta_{DH} + \frac{m_{bark} \cdot HHV_{bark} + m_{dust} \cdot HHV_{dust}}{m_{biomass} \cdot HHV_{biomass}} \qquad (21)$$

where η – efficiency, m – mass flow rate [kg/h], HHV – higher heating value [MJ/kg dry]. Bark and sawdust (assuming the same composition and heating value as woodchips) are also taken into account when calculating the overall heat utilization efficiency. Note that the overall efficiency do not include district heat negative efficiency, the meaning with showing (later) a negative efficiency for district heat is to show that additional external heat is required to supplement the district heat plant, or alternatively the bark and sawdust could be burned to maintain the heat production. As shown in Figure 10, the model predicts higher energy efficiency in the low temperature range (300 – 350 °C), however the quality of the biocarbon mimics torrefaction quality, which is below 66% fixed carbon content. Overall heat utilization efficiency decreases almost linearly with increasing pyrolysis temperature. There is a strong influence of feedstock moisture content on the overall heat utilization efficiency (Figure 10); increasing moisture content means a higher energy consumption for drying. Increasing pressure also increases the heat utilization efficiency due to increasing biocarbon yield.

4. Techno – economic analysis (TEA)

The next stage of the model is techno – economic analysis, which allows estimating the costs associated with production of biocarbon as a function of three parameters: scale of production and process temperature and pressure. Aspen Plus results developed for the base case (10 TPD) is based on a fresh logwood moisture content of 40%. TEA analysis is conducted based on the hierarchical three factors simulation coupled to cost parametric analysis. Four different scenarios are identified to analyze the biocarbon value chain. Statistical simulation experiments (Box – Behnken approach) have been used for simulation of experimental design and the results of mass and energy balances for each scenario are used as input to the cost modeling. Parametric cost modeling functions are developed using the cost models based on the three factors Box-Behnken approach. The obtained results were used to assess economic viability. The TEA modelling method is described in the flowchart shown in Figure 11.

4.1 Scenario description

Four scenarios are identified for the biocarbon value chain studies as shown in

Table 5.

Scenario A is based on the transport of logwood from the forest to the plant as shown in Figure 12. In this scenario, logwood handling is considered similar to the pulp and paper industries' practices. The feedstock is fresh logwood that is processed in the plant's wood handling zone involving storage, debarking, chipping and drying, followed by the carbonization and CHP. Here in this case, pyrolysis vapors, both non-condensable gases and condensable hydrocarbons are burnt in the CHP plant. The main product of this scenario is biocarbon. Electricity and district heat are co-products. After internal utilization of steam to the plant for woodchips drying, the excess heat generated can be sold to nearby industrial cluster office buildings.

In Scenario B, shown in Figure 13, the woodchips are transported to the plant gate and it is investigated how far the production cost of biocarbon deviate from scenario A. The wood handling process steps are woodchips storage and drying (debarking and chipping are eliminated). All other steps remain the same as in scenario A. The main product is biocarbon, co-products are electricity and district heat.

In Scenario C the CHP plant is eliminated as shown in Figure 14. Here the pyrolysis vapors are quenched in the condenser to produce the biooil and this will be sold as a co-product.

This is the post-print version.
Published version dx.doi.org/10.1021/acs.energyfuels.6b03441

The feedstock is fresh logwood that is processed in the plant pretreatment zone. Pyrolysis gas is burnt in a gas burner and heat is supplied to the dryer and pyrolysis reactor by indirect heat exchangers. Excess heat required for the dryer is supplied by the external heat supply (e.g. burning the bark and sawdust). As well, additional electricity required for the process is supplied from the grid. This makes sense as rather cheap electricity is available from the Norwegian hydropower dominated electricity grid. The main products are biocarbon and biooil. The price for biooil (tar) is set to 500$/ton according to market price. There is possibility to cut down Norwegian wood tar import. According to the statistics, the annual wood tar import is 250 tons [32], which is a small amount. However, there are other alternative markets for tars/biooil, for example extraction of valuable chemicals.

Scenario D is a copy of scenario A with a change of compression gas. Air is used instead of nitrogen as it is used in Flash Carbonization^{TM} by Antal et al. [29, 30]. This will reduce the costs associated with the supply of nitrogen. The scenario configuration is shown in Figure 15.

4.2 Purchase equipment and installation costs

This is the post-print version.
Published version dx.doi.org/10.1021/acs.energyfuels.6b03441

The purchase equipment cost is defined as

$$C_{TPEC,i} = C_{S_b,I_b}(S/S_b)^g \quad (22)$$

where $C_{TPEC,i}$ is the purchase equipment cost in $ evaluated for each equipment i, C_{S_b,I_b} is the base year purchase equipment cost in $ for base-case equipment size S_b (arbitrary unit), g is the equipment scale index, S is actual equipment size (in the same arbitrary unit) based on scale specification.

The purchase equipment and installation cost were evaluated based on the function defined by Kempegowda et al. [33, 34], which is a modified version of the Guthrie-Ulrich method [35], and includes pressure, materials and required auxiliary systems, i.e., electric system, piping and valves, instrumentation and control, through simple multiplication factors.

The purchase equipment and installation cost in $ for each equipment i is defined as:

$$C_{S,I,i} = f_{overall} C_{TPEC,i}(I/I_b)k_t^{n-n_b} \quad (23)$$

where the cost index I (arbitrary unit) used in this study is based on the Chemical Engineering Plant Cost Index (CEPCI). It is updated for the year 2015 and I_b is the cost index (in same arbitrary unit as I) in the base year, $k_t^{n-n_b}$ is the train cost factor since the n^{th} train is relatively cheaper than the train number n_b of the reference base case because both can use part of the auxiliary equipment, the parameter k_t is assumed to 0.9 [36]. Overall installation factor is

$$f_{overall} = f_{mat} f_p f_{inst} \quad (24)$$

where f_P is the pressure factor, f_{mat} is the material factor and f_{inst} is the installation factor. The installation factor varies based on the type of equipment in the process value chain. This is evaluated based on equation 25.

$$f_{inst} = 1 + f_M[1 + (L/M)k_L] \quad (25)$$

This is the post-print version.
Published version dx.doi.org/10.1021/acs.energyfuels.6b03441

with f_M and (L/M) representing installation module factor and labor to module cost ratio and $k_L = 1.47$ is the labor factor for Norway. Coefficients for each process equipment were used based on Wood et al. [37].

Overview of process equipments for the Aspen Plus base scale is shown in

Table 6.

This is the post-print version.
Published version dx.doi.org/10.1021/acs.energyfuels.6b03441

The cost calculation for the dryer is based on the surface area of each stage in accordance with equation 26.

$$C_{dryer} = h(15000 + 10500A_d) \quad (26)$$

where A_d is the surface area of the dryer in m^2 and h is the number of stages. The cost is calculated in \$ in base year 1998. Other factors are presented in

This is the post-print version.
Published version dx.doi.org/10.1021/acs.energyfuels.6b03441

Table 6. The cost of the carbonization reactor is calculated based on the weight of vessels, assuming three hot reactors, whereof one heating and one cooling section are used to ensure the continuity of the process. The cost of each reactor is equal

$$C_{reactor} = 73 f_{cp} {W_v}^{0.66} \mu \quad (27)$$

where f_{cp} is the cost factor, W_v is the weight of one vessel in kg, μ is the total number of vessels. The cost is calculated in $ in base year 2002. Other factors are presented in

Table 6. As well,

Table 7 presents the base scale TPEC costs for the different scenarios based on the cost components involved in the process chains. Purchase equipment cost decreased significantly for scenario C, due to removal of the CHP unit. TPEC for scenario A and D is the same because there is only a change in pressurizing medium.

4.3 Total permanent investment

This is the post-print version.
Published version dx.doi.org/10.1021/acs.energyfuels.6b03441

The total permanent investment [$] include the cost components outside the battery limit (OSBL). These are coupled to purchase equipment installation factors through equation 28. This is based on the work of Kempegowda et al. [33].

$$C_{TPI} = \left(\sum_i C_{S,I,i}\right)\left[1 + f_{site} + f_{building} + f_{land}\right]\left[1 + f_{cont} + f_{eng}\right]\left[1 + f_{dev} + f_{com}\right] \quad (28)$$

where $\left(\sum_i C_{S,I,i}\right)$ is the total purchase and installation cost in $, for the overall plant, and f_i represent additional costs factors including civil work associated with site preparation and process-equipment building, offsite accessibility and services, contingency margin, contractors, land, royalties and patents. Cost factors are shown in

Table 8. Cost associated factors to estimate the Total Permanent Investment (TPI) [33]

Factor	Cost associated factors	Typical value	Adopted value
fsite	Site preparation	0.05 – 0.2	0.05
fbuilding	Buildings	0.05 – 0.1	0.05
fland	Land	0.05 – 0.1	0.05
fcont	Cost of contingency	0.05 – 0.15	0.05
feng	Engineering	0.02 – 0.05	0.02
fdev	Project development and	0.02 – 0.03	0.02
fcom	Commissioning	0.1	0.1

This is the post-print version.
Published version dx.doi.org/10.1021/acs.energyfuels.6b03441

.

TPEC is only one part of the total costs associated with plant construction, as shown in Table 7. According to Timmerhaus et al. [38] total purchase and installation cost is typically 4 – 5 times higher than TPEC for solids processing. In this model the ratio is around 4.5.

4.4 Operating expenses

This is the post-print version.
Published version dx.doi.org/10.1021/acs.energyfuels.6b03441

The operating expenses (OPEX) in \$ per annual basis are calculated from

$$C_{OPEX} = C_B + C_{op,d} + C_{op,i} + C_{labor} \tag{29}$$

where C_B is cost of biomass supply, $C_{op,d}$ represents the total direct variable, operational dependent on the annual biomass to biocarbon conversion, $C_{op,i}$ is the fixed indirect operational costs not directly dependent on the amount of biomass processed but required for having the plant in activity, and C_{labor} is the labor cost.

Labor cost in \$ is calculated based on the exponential function of employed people $E_{ppl,i}$ and appropriate annual salaries D_i in \$ according to equations 30 and 31.

$$C_{labor} = \sum_i E_{ppl,i} D_i \tag{30}$$

$$E_{ppl,i} = \left(\frac{P_{act}}{P_{base}}\right)^{b_i} \tag{31}$$

where P_{act} is actual biocarbon production in TPD, P_{base} = 10 TPD. Base scale labor costs and their scaling factors are presented in Table 9.

The reference values for the fixed indirect operational costs $C_{op,i}$ are shown in

Table 10. The direct variable operational cost $C_{op,d}$ depends on the used media and the produced wastes, which are proportional to annual plant operating time. The cost of biomass supply in \$ can be estimated from

$$C_B = \left(\dot{M}_F t_{prod} / \rho_B\right)\left[c_{expl} + c_{chip} + c_{tr,f} + c_{tr,L} L_f\right] \tag{32}$$

where $\dot{M}_F$ indicates the plant capacity [kg/h] based on the input biomass mass flow rate, t_{prod} is the annual production time [hours], ρ_B is the input biomass density [kg/m^3], c_{expl} is the forest exploitation cost per unit volume of biomass [\$/m^3], c_{chip} is the cost for biomass chipping and storage per unit volume of biomass [\$/m^3], $c_{tr,f}$ is the fixed transport costs per unit volume of biomass [\$/m^3] and $c_{tr,L}$ is the variable (distance-dependent) transport costs per unit volume and transport distance of biomass [\$/m^3/m] and

$$L_f = 2\left(\dot{M}_F t_{prod}/m_{f,S}\right)^{1/2} \quad (33)$$

is the average biomass transport distance [m], which depends on the annual biomass conversion of the plant, with $m_{f,S}$ as the biomass production per unit area [kg/m^2].

Annual base scale 10 TPD OPEX for the different scenarios is shown in Table 11. Visible differences in the costs arise from the various scenario configurations. In scenario B cost of biomass supply is higher because woodchips used as feedstock is more expensive than logwood. The lowest OPEX is in Scenario D, where air is used instead of expensive nitrogen to pressurize the pyrolysis reactor. Scenario C is characterized by the highest operating expenses due to removal of the CHP unit. The excess heat and electricity must then be purchased externally.

Biomass supply cost comparison: Biomass supply under Norwegian conditions is the largest share of OPEX together with labor cost, as shown in Table 11. Biomass supply variables under Norwegian conditions are shown in Table 12. Two different feedstocks (spruce logwood and spruce woodchips) were compared at different operating conditions (temperature and pressure) and scale of biocarbon production. Replacement of logwood for woodchips resulted in an increased cost in the supply of biomass by 18%, which is independent of the operating conditions. With the increasing of operating pressure from 1 to 10 bar, there is a decrease of biomass supply cost of around 11% in the carbonization temperature range of 450 – 500 °C and at a biocarbon production of 45 – 60 TPD. This attribute is common for all cases, and this is due to the increased yield of biocarbon at elevated pressure in the carbonization temperature range. The details of biomass supply cost in MM$/year for various carbonization conditions are supplemented as Appendix E.

$$\text{Biomass cost} = x_0 + Tx_T + px_p + Wx_W + T^2x_{TT} + p^2x_{pp} + W^2x_{WW} + Tpx_{Tp} + TWx_{TW} + pWx_{pW} \quad (34)$$

This is the post-print version.
Published version dx.doi.org/10.1021/acs.energyfuels.6b03441

where T is temperature in °C, p is pressure in MPa in this equation, W is scale of biocarbon production in TPD, and the x coefficients for logwood and woodchips are shown in Table 13.

Influence on the overall OPEX: Figure 16(a) and (b) shows the influence of operating conditions pressure and temperature versus plant scale on the overall operating expenses. Generally, all cases showed increasing trend for OPEX. Scenario B has higher OPEX, which is due to higher price of woodchips (284 NOK/m^3) supplied to the plant compared to logwood (236 NOK/m^3). It also depends on the biomass share of total operating expenses. The difference is around 7 – 8.5% (450 – 500 °C, 1 – 10 bar and 60 TPD). In scenario A increasing pressure from 1 to 10 bar increases OPEX by 6 – 8% (450 – 500 °C and 40 – 60 TPD). Scenario C gives higher OPEX than scenario A, around 50 – 55% increase in the cost of biocarbon is estimated. This is due to purchase of heat and electricity for the auxiliary utilities in the plant.

4.5 Economic viability

Economic viability analysis is carried out for the four scenarios described in section 4.1. Impact of different process configurations, operating conditions (temperature in the range 300 – 500 °C and pressure in the range 1 – 10 bar) and scale of biocarbon production (10 – 60 TPD). The results were compared based on the relative difference between scenarios B, C, D and reference scenario A according to equation 35.

$$RD_{\%} = \frac{R_i - R_A}{R_A} \cdot 100 \qquad (35)$$

where $RD_{\%}$ is the relative difference in percent, R_i is the result for scenario i (i = B, C, D), R_A is the result for reference scenario A.

Financial parameters are gathered in Table 14. Economic viability is calculated based on 20 years plant lifetime with plant operating factor 85% (7446 hours/year). The equipment is

This is the post-print version.
Published version dx.doi.org/10.1021/acs.energyfuels.6b03441

depreciated according to a straight line depreciation model during a 20 years period. The investment is financed 30% by equity and 70% by loan. Loan repayment period is set to 10 years with 7% interest rate. The total permanent investment cost (TPI) is updated to US$ (2015) based on Chemical Engineering Plant Cost Index (CEPCI 2015). According to Norwegian condition income tax rate is 28%.

Specific plant cost comparison: Specific plant cost TPEC/kW biocarbon output is the cost associated with the purchased equipments expressed as the cost per unit of product output. Influence of carbonization process conditions (pressure and temperature) on the TPEC versus various plant capacities are shown in Figure 17(a), (b) and (c). TPEC follows the scale of economics rules and shows decreasing trend with increasing plant capacity [33]. Scenario B is around 1 – 8% cheaper compared to scenario A, this is due to scenario A having more functional units for handling the logwood (debarker and chipper).

Influence of pressure: Elevated pressure in the reactor decreased TPEC, increasing pressure from 1 to 10 bar (Figure 17(a)) decreases the TPEC around 10% in the temperature range of 450 – 500 °C and for 60 TPD. This attribute is due to the increased biocarbon yield at elevated pressures. TPEC for scenario C is decreasing relatively to scenario A, the cost reduction is around 5 – 6% for 10 bar, 450 – 500 °C and 60 TPD and 12% for 1 bar, 450 – 500 °C and 60 TPD. The reason for such decrease is elimination of the CHP unit in scenario C and production of biooil as a co-product. Pyrolysis gases are burnt in the gas burner and produced heat is utilized for the drying and pyrolysis reactor. The associated cost is based on the burner configuration rather on the complete CHP unit. Scenario D is not shown because it has the same cost as Scenario A, the difference is only in OPEX (air instead of nitrogen).

Influence of temperature: Similarly, influence of carbonization temperature (300 °C to 500 °C) on TPEC are shown in Figure 17(b) and (c). Increasing temperature increases the plant specific TPEC, which is due to a decreasing biocarbon yield at the same pressure, shown for

This is the post-print version.
Published version dx.doi.org/10.1021/acs.energyfuels.6b03441

677 1 bar in Figure 17(b) and 10 bar in Figure 17(c). TPEC almost doubles at high temperature, however, the quality of biocarbon produced at low temperature carbonization may not be suitable to replace coke as a reductant, which is due to the high volatiles content and the low fixed carbon content.

Cost of biocarbon: Cost of biocarbon [$/GJ] is evaluated over the entire lifetime of the plant, assuming that the project is financed 100% from loan, and is calculated from equation 36.

$$C_{biocarbon} = \frac{\sum_{u=1}^{U}[\beta^{u}(C_{TPi,u}+C_{OPEX,u}-C_{IN,u})]}{\sum_{u=1}^{U} HHV_{biocarbon} \cdot p_{bc,u}} \quad (36)$$

where u is the year starting from the plant construction, U is the plant lifetime in years, $\beta = 1/(1+r)$ is the discount factor which represents time value of money, r is the interest rate. $C_{TPi,u}$ is the annual permanent investment cost in \$, $C_{OPEX,u}$ is the annual operating expenses in \$, $C_{IN,u}$ is the annual income in \$ from selling co-products (electricity, heat, bark, sawdust and CO_2 replacement), however, in our TEA analysis, the bark and sawdust are not included in the evaluation. $HHV_{biocarbon}$ is the HHV of produced biocarbon [MJ/kg dry biocarbon], $p_{bc,u}$ is the annual biocarbon production [ton]. The annual operational income in $ is calculated from equation 37.

$$C_{IN,u} = C_{el,u} + C_{heat,u} + C_{CO2,u} \quad (37)$$

where $C_{el,u}$ is annual income in \$ from selling electricity, $C_{heat,u}$ is annual income in \$ from selling heat, $C_{CO2,u}$ is annual income in \$ from replacement of fossil fuel to renewable based on avoided CO_2 emission. Reference values are shown in Table 15.

Influence of operating conditions on the cost of biocarbon: The cost of biocarbon is the decision parameter for evaluating the economic viability of the biocarbon production scenarios based on the current market conditions. The economic viability is estimated for the scenarios A, B, C and D at operating temperatures 300 – 500ºC and pressures 1 – 10 bar and for scale of biocarbon production of 10 to 60 TPD. The results are shown in Figure 18, Figure 19 and Figure 20.

Increasing pressure from 1 bar to 10 bar in Scenario A results in increased biocarbon cost (Figure 18). The increase is ~10% in the lower temperature range (300 °C) where the price increased from ~10.5 $/GJ to ~11.5 $/GJ and ~1.5% at a temperature of 500 °C where the price increased from ~14 $/GJ to ~14.3 $/GJ, which is at the production scale of 50 – 60 TPD (Figure 18). Similar costs were estimated for Finnish conditions for torrefaction and for charcoal production[39]. Increasing pressure in the carbonization reactor at high temperature carbonization does not increase the cost significantly (Figure 18), this is due to the higher yield of biocarbon with increasing pressure.

Scenario C shows a large decrease in the production cost of biocarbon compared to scenario A (Figure 18), around 40 – 44% (**1 bar**, 450 – 500 °C and 40 – 60 TPD) the estimated price is ~8 $/GJ and around 30 – 36% (**10 bar**, 450 – 500 °C and 40 – 60 TPD) the estimated price is ~9.3 $/GJ. This is due to the advantage of co-production of biooil at the market price 500 $/ton. Increasing pressure in this case results in decrease of biooil yield, according to secondary pyrolysis reactions, which results in higher biocarbon and gas yields.

Supply of woodchips to the plant is increasing the cost of biocarbon for scenario B as shown in Figure 19. In comparison to the logwood purchasing scenario, there is direct purchase of woodchips to the plant at higher cost, the relative difference of production cost is around 5% compared to scenario A (**1 bar**, 450 – 500 °C and 55 – 60 TPD) with biocarbon price ~14.5 $/GJ and around 4% higher compared to scenario A (**10 bar**, 450 – 500 °C, 55 – 60 TPD) with biocarbon price 14.7 $/GJ. An interesting observation is that for the base scale, where the production is 10 TPD and the temperature range below 400 °C, there is an advantage of woodchips purchase to the plant by ~1% decrease in production cost (Figure 19), the biocarbon price is ~18 $/GJ. However, the grade of biocarbon produced at these conditions

Published version dx.doi.org/10.1021/acs.energyfuels.6b03441

is not suitable for metallurgical industries, this is because of the low fixed carbon content in the product.

When air is used to pressurize the reactor (scenario D), there is a decrease in biocarbon production cost of around 8% (Figure 20) compared to scenario A at 1 bar and scenario D at 10 bar at 500 °C and production scale 60 TPD, where the price is reduced from ~14 $/GJ to ~13$/GJ, Figure 20. This attribute is due to the compression energy consumption differences.

<u>Influence of biomass transportation distance:</u> Scenario A and D are considered for studying the influence of transport distance. Modelling results suggests that a carbonization temperature of 500 °C is suitable to achieve highest fixed carbon content (81%) [26]. Thus, the obtained biocarbon can be widely used in metallurgical industry as a reductant. In order to minimize the cost of production, a scale of production of 60 TPD is chosen for transportation cost analysis. The influence of biomass transportation distance on biocarbon production cost is shown in Figure 21Figure 21.

The cost of logwood is increasing with transportation distance according to a linear correlation. Under Norwegian conditions fresh woody biomass costs 4.75 $/GJ for a 20 km transportation distance and it is increasing up to 7.15 $/GJ when the transportation distance is 220 km, Figure 21(a). Therefore, it is reasonable to transport biomass up to several tens of kilometers. The plant location should be properly selected to avoid additional cost and emissions related with biomass transportation. Figure 21(b) shows the influence of biomass transport on biocarbon production cost for scenario A and Figure 21(c) for scenario D. Increasing pressure additionally increases the cost of biocarbon production.

<u>Economic viability on selling price of biocarbon product</u>**:** Internal rate of return (IRR) is used as a financial viability indicator to analyze the project viability. It is defined as the discount rate that would make the net present value (NPV) of the investment equal to zero.

This is the post-print version.
Published version dx.doi.org/10.1021/acs.energyfuels.6b03441

Project IRR for scenario A, B and C is selected for analyzing the (500 °C, 60 TPD biocarbon production) economics at 70% debt as shown in Figure 21(d). The highest IRR achieves scenario C, where biooil is a co-product, it is due to high market price of woody tar at 500$/ton. The IRR decrease at elevated pressure according to lower biooil yield. The difference between scenario A and D is related to the difference in pressurizing agent (nitrogen and air).

5. Conclusions

Detailed simulation of the biocarbon production value chain consisting of logwood handling, debarking, chipping, drying, carbonization, and combined heat and power production plant was developed using Aspen Plus. Carbonization process yields (product yields) are predicted with a multifunctional model considering pressure, temperature and particle size effects. The empirical correlation indicates a strong influence of temperature as well as a significant influence of pressure and particle size on the biocarbon yield. As well, biocarbon energy efficiency is higher in the low temperature carbonization regime, however, the biocarbon quality with respect to fixed carbon content is lower in the low temperature carbonization regime. For high temperature carbonization, above 400ºC, increasing pressure in the carbonization reactor increases the fixed carbon yield.

Feedstock moisture content has strong influence on district heat efficiency. For the fresh wood having 60% moisture, both district heat efficiency and steam export is negative, since all the low-pressure steam is consumed for thermal drying of the feedstock, which has a penalty of 5-10% of the HHV of input feedstock. A parametric function for district heat production is developed for the carbonization process parameters (temperature, pressure) and production scale. Techno-economic analysis was conducted for the four case scenarios, Scenario A is based on logwood transport from the forest to the plant gate with biocarbon as

This is the post-print version.
Published version dx.doi.org/10.1021/acs.energyfuels.6b03441

the main product and district heat and electricity as the co-products. Scenario B is based on the supply of woodchips to the plant with biocarbon as the main product and district heat and electricity as the co-products. Scenario C is based on the biocarbon as a main product and biooil as co-product. In Scenario D nitrogen is replaced with air as inert agent air in the carbonization reactor.

A novel approach for a parametric cost modelling function for the overall plant design is developed based on a statistical approach using the Box and Behnken technique to the study the influence of scale and operating variables (temperature and pressure). TEA reveals that specific plant cost (TPEC) can be reduced by reducing wood handling (scenario B) by supplying woodchips in the range of 1-8% in comparison to scenario A. Also, there is a decrease in total purchase equipment cost (TPEC) with increasing pressure by (Scenario A) ~10% (from 1 to 10 bar, 450-500, 60 TPD), because of the higher pressure effect on the biocarbon yield. Moreover, increasing scale of production results in decreasing specific TPEC, which follows the scale of economics rule. Specific TPEC cost in Scenario C is decreased by 5-6% (for 10 bar, 450-500ºC, 60 TPD) and 12% (1 bar, 450-500ºC, 60 TPD) as compared to scenario A. The major share of OPEX is the biomass feedstock price. Overall OPEX cost is higher in scenario B where woodchips are purchased at market rate. The difference is around 7-8.5% (450-500ºC, 1-10 bar, 50-60 TPD). In Scenario A, increasing pressure from 1 bar to 10 bar increased OPEX ~6-8% (450-500ºC, 40-60 TPD). Scenario C gives higher OPEX than scenario B, around 50-55% due to purchase of heat and electricity.

Cost of biocarbon production ($/GJ) is higher in Scenario B than Scenario A by ~5% (1 bar, 450 -500ºC, 55-60 TPD) and ~4% (10 bar, 450-500ºC, 55-60 TPD). There is an advantage of woodchips purchase by ~1% regarding production cost at lower scale for the base scale of 10 TPD and carbonization temperature below 400ºC. In Scenario A increasing pressure from 1 bar to 10 bar increased production cost of biocarbon ($/GJ), with ~9.7% at a

This is the post-print version.
Published version dx.doi.org/10.1021/acs.energyfuels.6b03441

temperature of 300ºC and 1.3% at 500ºC, both in the production range of 50-60 TPD, which can be regarded as insignificant.

Scenario C, with biooil as co-product, exhibits a large decrease in the production cost of biocarbon ($/GJ) of 40-44% (1 bar, 450-500ºC, 40-60 TPD) and 30-36% (10 bar, 450-500ºC, 40-60 TPD).

However, increasing the pressure from 1 bar to 10 bar decreased the yield of biooil due to increased biocarbon yields at elevated pressure. Under Norwegian conditions, supply of woodchips instead of logwood to the plant gate increases the supply cost of biomass by 18% (independent of the operating conditions).

Cost of biomass supply increased from 4.75 $/GJ to 7.15 $/GJ by increasing the transportation distance of logwood supply from forest to the plant gate from 20 to 220 km. This also suggest that cost of biocarbon production increase linearly at a rate of 0.5 $/GJ for every 40 km transport distance for the best selected case for metallurgical industry (60 TPD at 500ºC). Case D with pressurization of the carbonization reactor with air decreased the cost of biocarbon by ~1 $/GJ in comparison with nitrogen at the same operating conditions. Pressurization by air reduced the cost of biocarbon by 0.5 $/GJ at 5 bar and 1 $/GJ at 10 bar for the same transport distance of forest logwood. Finally, the economic return based on IRR suggests that highest IRR achieved for scenario C, where biooil is a co-product, which is due to high market price of woody tar at 500 $/ton. Finally, the TEA reveals the influence of different grades of biocarbon, i.e. different fixed carbon contents, for metallurgical and cofiring applications. Higher grades of biocarbon increases the cost of production of biocarbon, however, for metallurgical industries a relatively high grade is needed.

Acknowledgements

The authors acknowledge the financial support from the Research Council of Norway, and the industrial partners (Elkem AS, Department Elkem Technology; Norsk Biobrensel AS; AT Skog SA; Eyde-nettverket; Saint Gobain Ceramic Materials AS; Eramet Norway AS; Alcoa Norway ANS) in the BioCarb+ project.

References

1. SSB Energy use in the manufacturing sector, Statistics Norway https://www.ssb.no/en/energi-og-industri/statistikker/indenergi/aar/2016-06-17
2. Scarlat, N.; Dallemand, J.-F.; Skjelhaugen, O. J.; Asplund, D.; Nesheim, L., An overview of the biomass resource potential of Norway for bioenergy use. *Renewable and Sustainable Energy Reviews* **2011,** 15, (7), 3388-3398.
3. Belbo, H.; Talbot, B., Systems Analysis of Ten Supply Chains for Whole Tree Chips. *Forests* **2014,** 5, (9), 2084-2105.
4. Lucas, L. H. M. Effect of pressure on the characteristics of biomass pyroysis. Ph.D thesis., University of Newcastle. Faculty of Engineering and Built Environment, School of Engineeri, 2012.
5. Mohan, D.; Pittman, C. U.; Steele, P. H., Pyrolysis of Wood/Biomass for Bio-oil: A Critical Review. *Energy & Fuels* **2006,** 20, (3), 848-889.
6. de Oliveira Vilela, A.; Lora, E. S.; Quintero, Q. R.; Vicintin, R. A.; Pacceli da Silva e Souza, T., A new technology for the combined production of charcoal and electricity through cogeneration. *Biomass and Bioenergy* **2014,** 69, 222-240.
7. Antal, M. J.; Mok, W. S. L.; Varhegyi, G.; Szekely, T., Review of methods for improving the yield of charcoal from biomass. *Energy & Fuels* **1990,** 4, (3), 221-225.
8. FAOSTAT Forestry Production and Trade. http://faostat3.fao.org/download/F/FO/E (25th August),
9. Antal, M. J.; Grønli, M., The art, science, and technology of charcoal production. *Industrial & Engineering Chemistry Research* **2003,** 42, (8), 1619-1640.
10. Demirbas, A., Carbonization ranking of selected biomass for charcoal, liquid and gaseous products. *Energy Conversion and Management* **2001,** 42, (10), 1229-1238.
11. Violette, M., Memoire sur les Charbons de Bois. *Ann. Chim. Phys* **1853,** 32, 304.
12. Antal, M. J.; Croiset, E.; Dai, X.; DeAlmeida, C.; Mok, W. S.-L.; Norberg, N.; Richard, J.-R.; Al Majthoub, M., High-yield biomass charcoal. *Energy & Fuels* **1996,** 10, (3), 652-658.
13. Wang, L.; Skreiberg, Ø.; Gronli, M.; Specht, G. P.; Antal, M. J., Is Elevated Pressure Required to Achieve a High Fixed-Carbon Yield of Charcoal from Biomass? Part 2: The Importance of Particle Size. *Energy & Fuels* **2013,** 27, (4), 2146-2156.
14. Van Wesenbeeck, S.; Wang, L.; Ronsse, F.; Prins, W.; Skreiberg, Ø.; Antal, M. J., Charcoal "Mines" in the Norwegian Woods. *Energy & Fuels* **2016**.
15. Deev, A.; Jahanshahi, S. In *Development of a pyrolysis technology to produce large quantities of charcoal for the iron and steel industry*, 6th International Congress on the Science and Technology of Ironmaking, 2012; 2012; pp 1132-1142.

This is the post-print version.
Published version dx.doi.org/10.1021/acs.energyfuels.6b03441

16. Jahanshahi, S.; Mathieson, J. G.; Somerville, M. A.; Haque, N.; Norgate, T. E.; Deev, A.; Pan, Y.; Xie, D.; Ridgeway, P.; Zulli, P., Development of Low-Emission Integrated Steelmaking Process. *Journal of Sustainable Metallurgy* **2015,** 1, (1), 94-114.
17. Brown, N. J.; Bastien, L. A. J.; Price, P. N., Transport properties for combustion modeling. *Progress in Energy and Combustion Science* **2011,** 37, (5), 565-582.
18. Peng, D.-Y.; Robinson, D. B., A New Two-Constant Equation of State. *Industrial & Engineering Chemistry Fundamentals* **1976,** 15, (1), 59-64.
19. Michael Suhr, e. a., Best Available Techniques (BAT) Reference Document for the Production of Pulp, Paper and Board. In Studies, I. f. P. T., Ed. European Commission: 2015.
20. Kollmann, F. F. P.; Kuenzi, E. W.; Stamm, A. J., Principles of Wood Science and Technology - II Wood Based Materials. **1975**.
21. Monsen, B.; Gronli, M.; Nygaard, L.; Tveit, H., The use of biocarbon in Norwegian ferroalloy production. **2001**

22. Laitila, J.; Asikainen, A.; Ranta, T., Cost analysis of transporting forest chips and forest industry by-products with large truck-trailers in Finland. *Biomass and Bioenergy* **2016,** 90, 252-261.
23. Johansson, A.; Fyhr, C.; Rasmuson, A., High temperature convective drying of wood chips with air and superheated steam. *International Journal of Heat and Mass Transfer* **1997,** 40, (12), 2843-2858.
24. Scheepers, G.; Wiberg, P.; Johansson, J., A method to estimate wood surface moisture content during drying. *Maderas. Ciencia y tecnología* **2017**, (AHEAD), 0-0.
25. Somerville, M.; Jahanshahi, S., The effect of temperature and compression during pyrolysis on the density of charcoal made from Australian eucalypt wood. *Renewable Energy* **2015,** 80, 471-478.
26. Neves, D.; Thunman, H.; Matos, A.; Tarelho, L.; Gómez-Barea, A., Characterization and prediction of biomass pyrolysis products. *Progress in Energy and Combustion Science* **2011,** 37, (5), 611-630.
27. Aslan, N.; Cebeci, Y., Application of Box–Behnken design and response surface methodology for modeling of some Turkish coals. *Fuel* **2007,** 86, (1), 90-97.
28. Noumi, E. S.; Blin, J.; Valette, J.; Rousset, P., Combined effect of pyrolysis pressure and temperature on the yield and CO2 gasification reactivity of acacia wood in macro-TG. *Energy & Fuels* **2015,** 29, (11), 7301-7308.
29. Antal, M. J.; Mochidzuki, K.; Paredes, L. S., Flash Carbonization of Biomass. *Industrial & Engineering Chemistry Research* **2003,** 42, (16), 3690-3699.
30. Antal, M. J. Flash Carbonization™ Process. http://www.hnei.hawaii.edu/node/219 (25th August),
31. Turnell, J. R.; Faulkner, R. D.; Hinch, G. N., Recent advances in Australian broiler litter utilisation. *World's Poultry Science Journal* **2007,** 63, (2), 223-231.
32. Bridgwater, A. V., *Advances in thermochemical biomass conversion*. 1994; Vol. 1.
33. Kempegowda, R. S.; del Alamo, G.; Berstad, D.; Bugge, M.; Matas Güell, B.; Tran, K.-Q., CHP-Integrated Fischer-Tropsch Biocrude Production under Norwegian Conditions: Techno-Economic Analysis. *Energy & Fuels* **2015,** 29, (2), 808-822.
34. Kempegowda, R. S.; Pannir Selvam, P.; Skreiberg, Ø.; Tran, K. Q., Process synthesis and economics of combined biomethanol and CHP energy production derived from biomass wastes. *Journal of Chemical Technology and Biotechnology* **2012,** 87, (7), 897-902.
35. Uhl, V. W., A guide to chemical engineering process design and economics, by Gail D. Ulrich, John Wiley & Sons, New York, Chichester, Brisbane, Toronto, Singapore “1984” 472 pages. $35.95. *AIChE Journal* **1984,** 30, (6), 1036-1036.
36. Larson, E. D.; Jin, H.; Celik, F. E., Large-scale gasification-based coproduction of fuels and electricity from switchgrass. *Biofuels, Bioproducts and Biorefining* **2009,** 3, (2), 174-194.
37. Woods, D. R., *Rules of Thumb*. 2007; p 478.
38. Peters, M. S.; Timmerhaus, K. D.; West, R. E.; Timmerhaus, K.; West, R., *Plant design and economics for chemical engineers*. 5th ed.; McGraw-Hill New York: 2003

Vol. 4.
39. Suopajärvi, H.; Pongrácz, E.; Fabritius, T., Bioreducer use in Finnish blast furnace ironmaking – Analysis of CO2 emission reduction potential and mitigation cost. *Applied Energy* **2014,** 124, 82-93.

This is the post-print version.
Published version dx.doi.org/10.1021/acs.energyfuels.6b03441

40. Hamelinck, C. N.; Faaij, A. P. C., Future prospects for production of methanol and hydrogen from biomass. *Journal of Power Sources* **2002,** 111, (1), 1-22.
41. Towler, G. P.; Sinnott, R. K., *Chemical engineering design: principles, practice, and economics of plant and process design*. Elsevier: 2013.

Nomenclature

$\dot{M}_F$	Plant capacity based on the input biomass mass flow rate (kg/h)
A_d	Dryer surface area (m^2)
b_i	Scaling factor (-)
C_{S_b,I_b}	Purchase cost of base scale equipment ($)
C_B	Cost of biomass supply ($)
C_B, $C_{op,d}$, $C_{op,i}$, C_{labor}, C_{OPEX}	Cost biomass, direct operating expenses, indirect expenses, cost of labor, annual operating expenses ($)
$C_{biocarbon}$	Cost of biocarbon ($/GJ)
c_{chip}	Biomass chipping and storage cost ($/m^3)
$C_{CO2,u}$	Annual income from replacement of fossil fuel to renewable based on avoided CO_2 emission ($)
C_{dryer}	Cost of dryer ($)
$C_{el,u}$	Annual income from selling electricity ($)
c_{expl}	Forest exploitation cost ($/m^3)
$C_{heat,u}$	Annual income from selling heat ($)
$C_{IN,u}$	Annual income from selling co-products ($)
$C_{OPEX,u}$	Annual operating expenses ($)
$C_{reactor}$	Cost of carbonization reactor ($)
$C_{S,I,i}$	Purchase cost of actual equipment ($)
$C_{TPEC,i}$	Total purchase cost of equipment ($)
$C_{TPI,u}$	Annual permanent investment cost ($)
C_{TPI}	Total permanent investment ($)
$c_{tr,f}$	Fixed transport cost ($/m^3)
$c_{tr,L}$	Variable transport cost ($/m^3/m)
D_i	Annual salaries ($)
$E_{ppl,i}$	Number of employed people
f_{cp}	Cost factor (-)

This is the post-print version.
Published version dx.doi.org/10.1021/acs.energyfuels.6b03441

f_M	Installation module factor (-)
f_{mat}, f_p, f_{inst}	Material factor, pressure factor, installation factor (-)
$f_{overall}$	Overall installation factor (-)
f_{site}, $f_{building}$, f_{land}, f_{cont}, f_{eng}, f_{dev}, f_{com}	Site factor, building construction factor, land factor, contingency factor, engineering factor, development fee, commissioning factor (-)
HHV_{bark}	Higher heating value of bark (MJ/kg dry)
$HHV_{biocarbon}$	Higher heating value of biocarbon (MJ/kg dry)
$HHV_{biomass}$	Higher heating value of biomass (MJ/kg dry)
HHV_{dust}	Higher heating value of dust (MJ/kg dry)
I_b	Base year cost index (same arbitrary unit as I)
k_L	Labor factor (-)
$k_t^{n-n_b}$	Equipment train factor (-)
L_f	Average biomass transport distance (m)
LHV_{Gas}	Gas lower heating value (MJ/kg)
m_{bark}	Mass flow rate of dry bark (kg/h)
$m_{biocarbon}$	Mass flow rate of dry biocarbon (kg/h)
$m_{biomass}$	Mass flow rate of dry biomass (kg/h)
m_{dust}	Mass flow rate of dry sawdust (kg/h)
$m_{f,S}$	Biomass production per unit area (kg/m^2)
$M_{IN-CHIP}$	Mass flow rate into the chipper (kg/h)
M_{LOG}	Logwood mass flow rate (kg/h)
n_b	Base case train cost factor (-)
P_{act}	Actual production (arbitrary unit)
P_{base}	Base scale production (same arbitrary unit as P_{act})
$p_{bc,u}$	Annual biocarbon production (ton)
P_{CH}	Power consumption chipper (kW)
P_{DE}	Power consumption for debarker (kW)
P_{el}	Electricity output from CHP (kW)
Q_{DH}	District heat thermal power (MJ/h)
$RD_{\%}$	Relative difference in percent
R_i	Result for scenario i (arbitrary unit)
R_A	Result for scenario A (same arbitrary unit as R_i)
S_b	Base equipment scale (same arbitrary unit as S)
S_{CH}	Static load Chipper (kg/h)
S_{DE}	Static load Debarker (kg/h)
t_{prod}	Annual production time (hours)
W_v	Weight of one vessel (kg)
X_{CH}	Chipper electricity consumption for static load (kW)
X_{DE}	Debarker electricity consumption for static load (kW)
$Y_{biocarbon}$	Biocarbon yield (kg/kg dry biomass)
$Y_{C,biomass}$	Carbon content in biomass (kg/kg dry ash free biomass)
$Y_{C,tar}$	Carbon content in tar (kg/kg dry tar)
$Y_{C,BC}$	Weight fraction of carbon in produced biocarbon, dry ash free basis (-)
Y_{CH4}	Gas yield of CH_4 (kg/kg dry ash free biomass)
Y_{CO}	Gas yield of CO (kg/kg dry ash free biomass)
y_{fC}	Fixed carbon yield (kg/kg dry ash free biomass)
$Y_{H,BC}$	Weight fraction of hydrogen in produced biocarbon, dry ash free basis (-)
$Y_{H,biomass}$	Hydrogen content in biomass (kg/kg dry ash free biomass)
$Y_{H,tar}$	Hydrogen content in biomass (kg/kg dry tar)
Y_{H2}	Gas yield of H_2 (kg/kg dry ash free biomass)
$Y_{O,BC}$	Weight fraction of oxygen in produced biocarbon, dry ash free basis (-)
$Y_{O,biomass}$	Oxygen content in biomass (kg/kg dry ash free biomass)
$Y_{O,tar}$	Oxygen content in biomass (kg/kg dry tar)
$Y_{overall}$	Overall heat utilization efficiency
Z_{cr}	Critical moisture content on dry basis (kg/kg)
Z_{eq}	Equilibrium moisture content on dry basis (kg/kg)
$\eta_{biocarbon}$	Biocarbon energy efficiency (MW biocarbon/MW biomass)
η_{DH}	District heat efficiency (MW district heat/MW biomass)
η_{el}	Electricity generation efficiency (MW electricity/MW biomass)
ρ_B	Input biomass density (kg/m^3)
μ	Number of vessels

Published version dx.doi.org/10.1021/acs.energyfuels.6b03441

A	Ash content in biomass (kg/kg dry biomass)
d	Particle diameter (mm)
FC	Fixed carbon content in biocarbon (kg/kg dry biocarbon)
g	Equipment scale index (-)
h	Number of dryer stages
I	Cost index (arbitrary unit)
L/M	Labor to module cost ratio (-)
n	Train cost factor (-)
p	Pressure (bar)
r	Interest rate
S	Actual equipment size (arbitrary unit)
T	Temperature (°C)
U	Plant lifetime in years
$v(\alpha)$	Normalized drying curve (-)
Z	Current moisture content on dry basis (kg/kg)
α	Normalized moisture content (-)
β	Discount factor
Subscripts	
i	Equipment index

List of Figures

This is the post-print version.
Published version dx.doi.org/10.1021/acs.energyfuels.6b03441

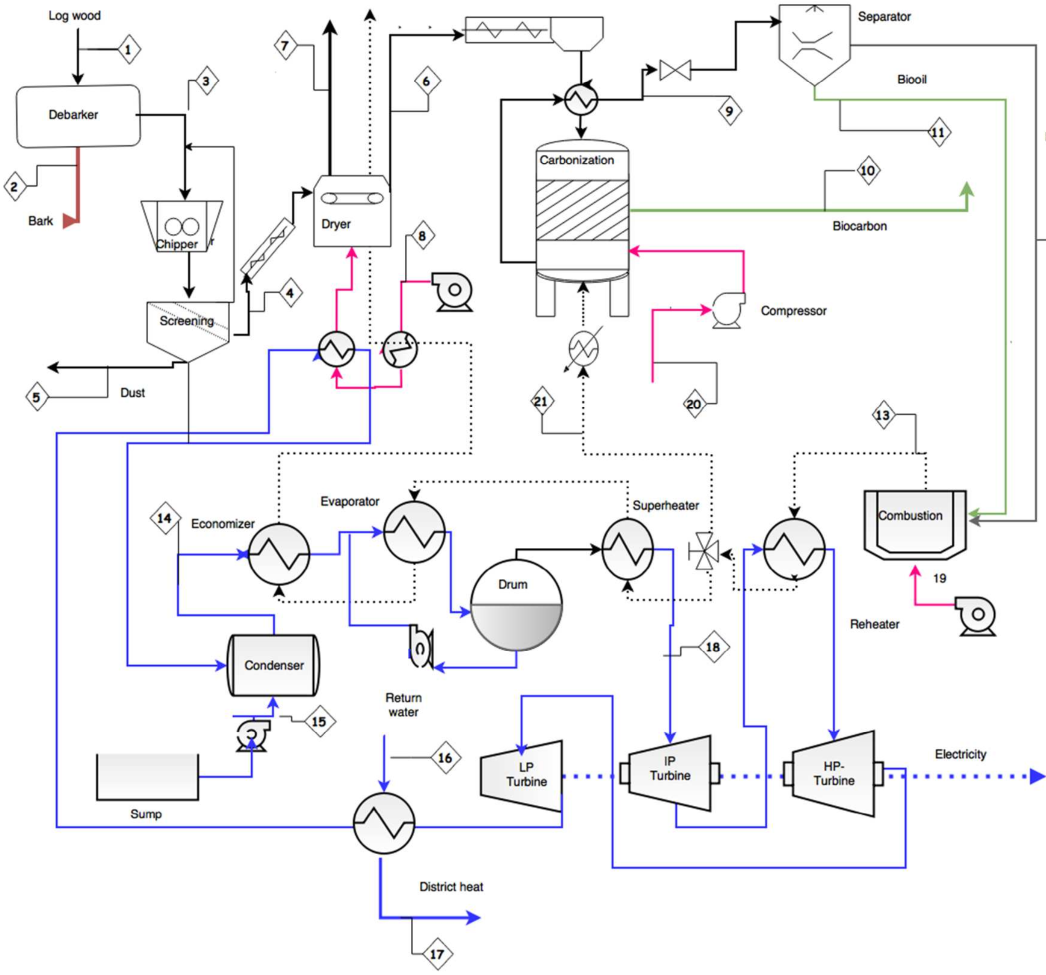

Figure 1. Biocarbon production process flow diagram

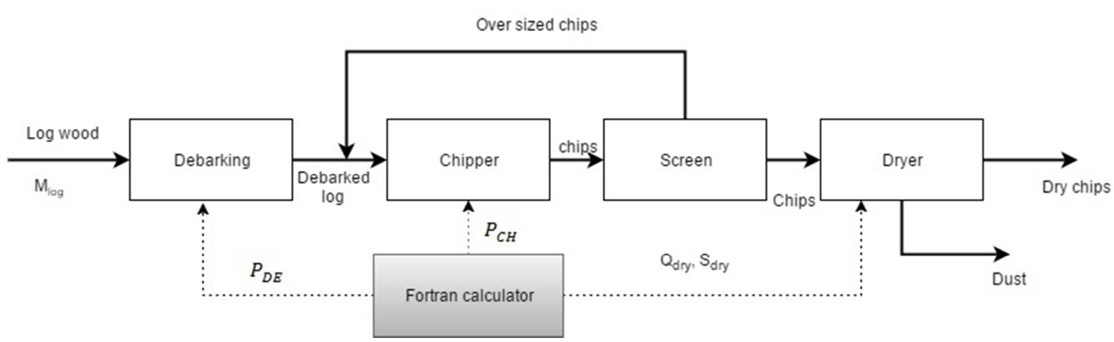

Figure 2. Aspen Plus model for logwood handling and thermal drying

This is the post-print version.
Published version dx.doi.org/10.1021/acs.energyfuels.6b03441

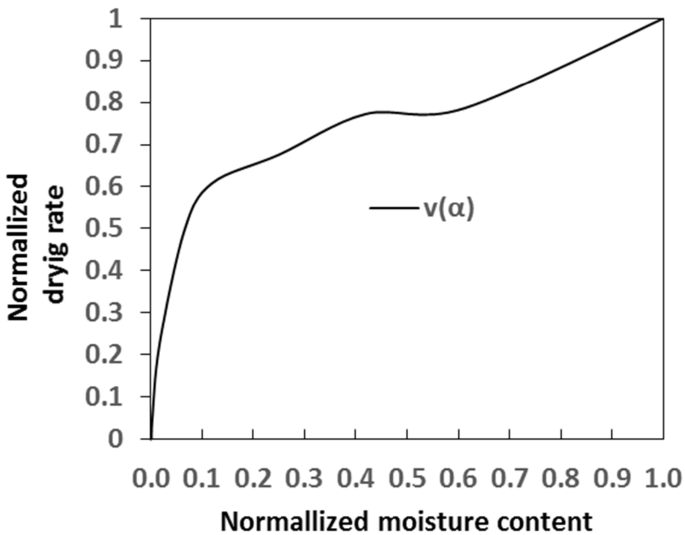

Figure 3. Normalized drying curve implemented in Aspen Plus model

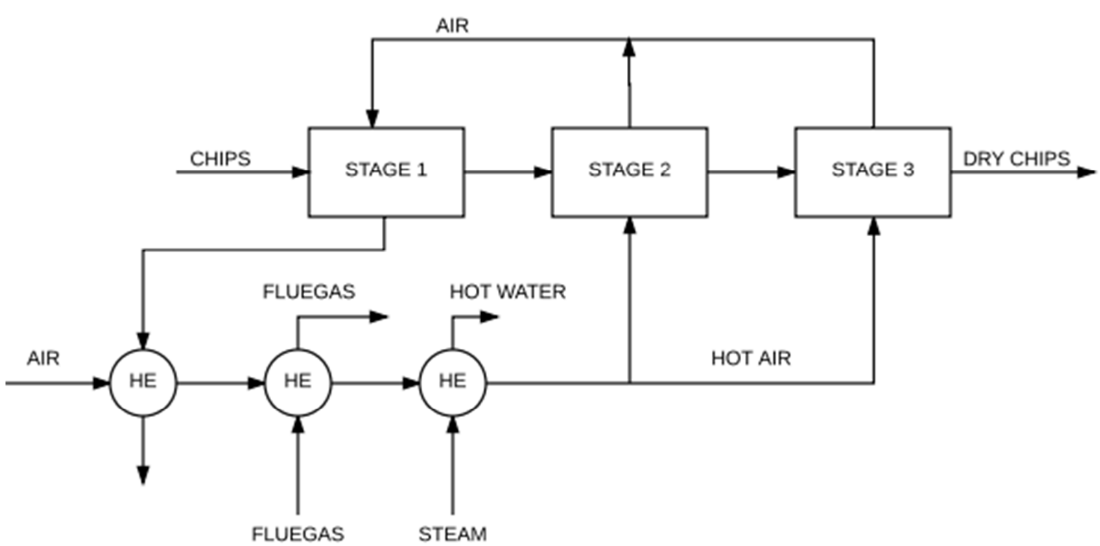

Figure 4. Staged drying model in Aspen Plus

This is the post-print version.
Published version dx.doi.org/10.1021/acs.energyfuels.6b03441

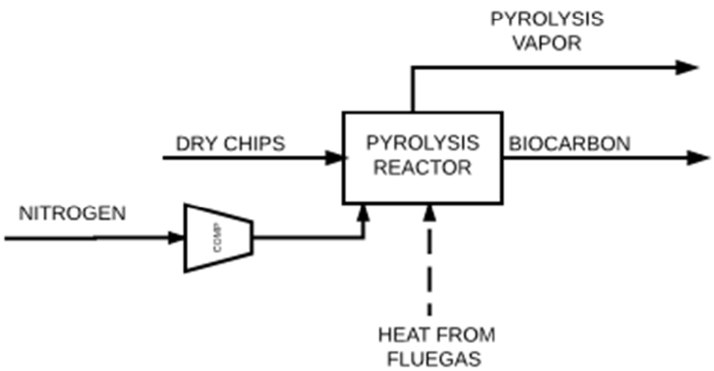

Figure 5. Simplified pyrolysis process flow diagram used in Aspen Plus

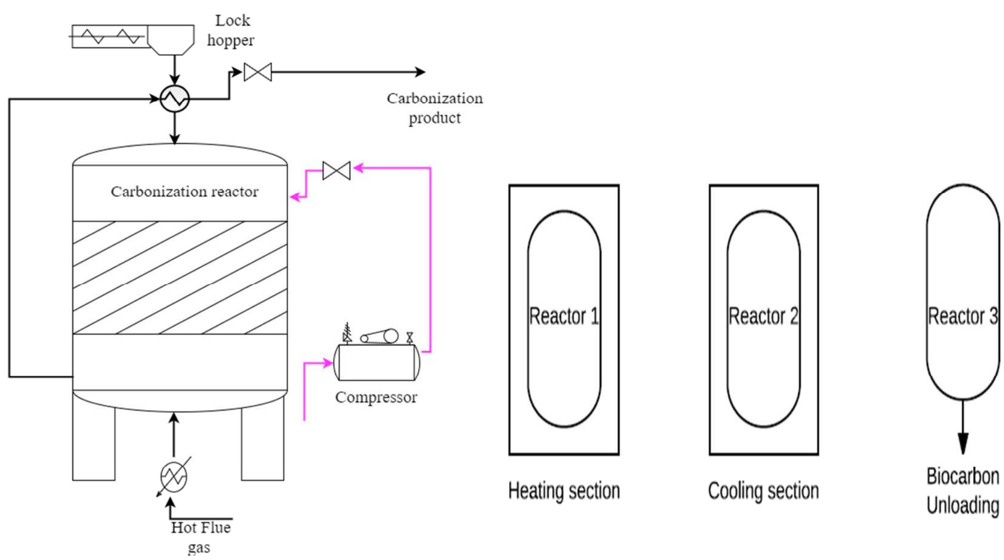

(a) (b)

Figure 6. Pyrolysis reactor (a) and schematic idea of reactor in semi-continuous operating configuration (b) - modified Antal design [30]

This is the post-print version.
Published version dx.doi.org/10.1021/acs.energyfuels.6b03441

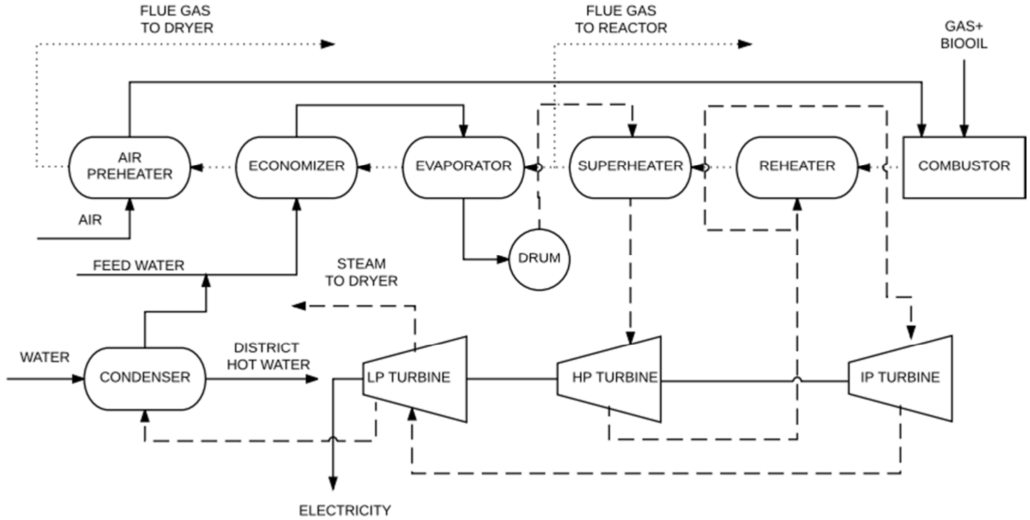

Figure 7. CHP process flow diagram

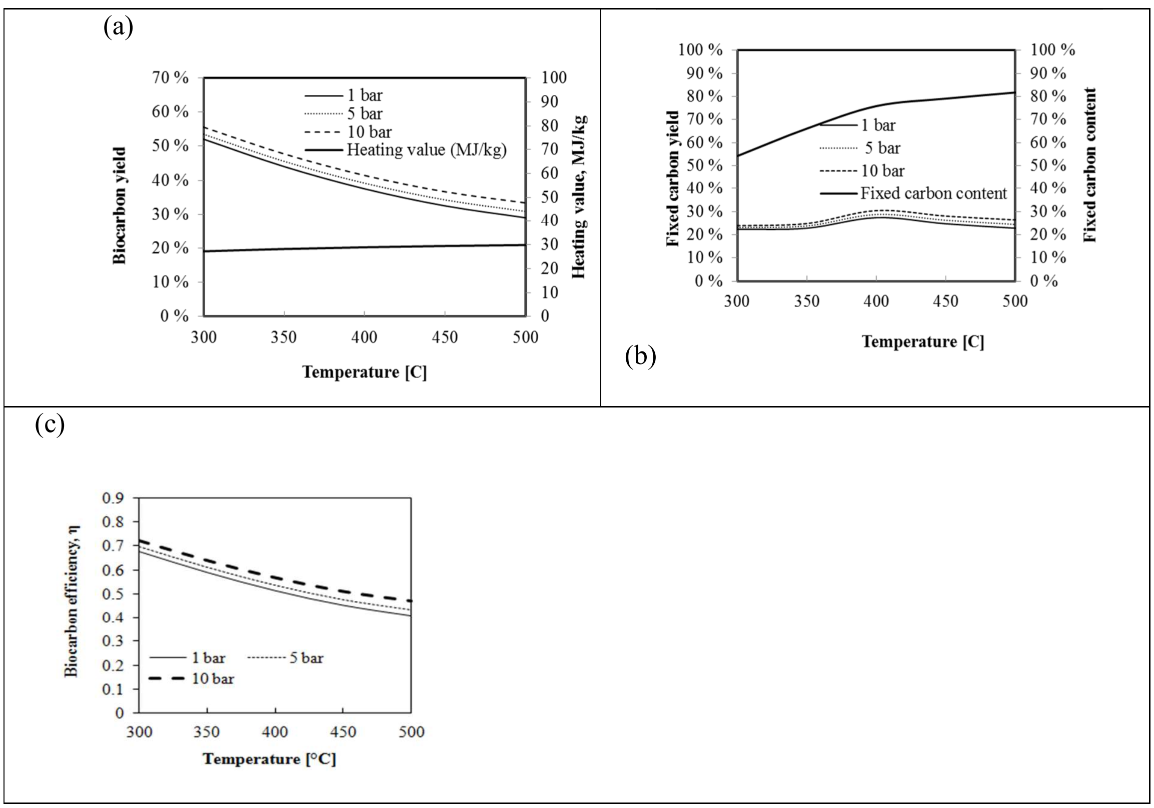

Figure 8. (a) Calculated biocarbon yield, (b) Fixed carbon yield, (c) Biocarbon energy efficiency

This is the post-print version.
Published version dx.doi.org/10.1021/acs.energyfuels.6b03441

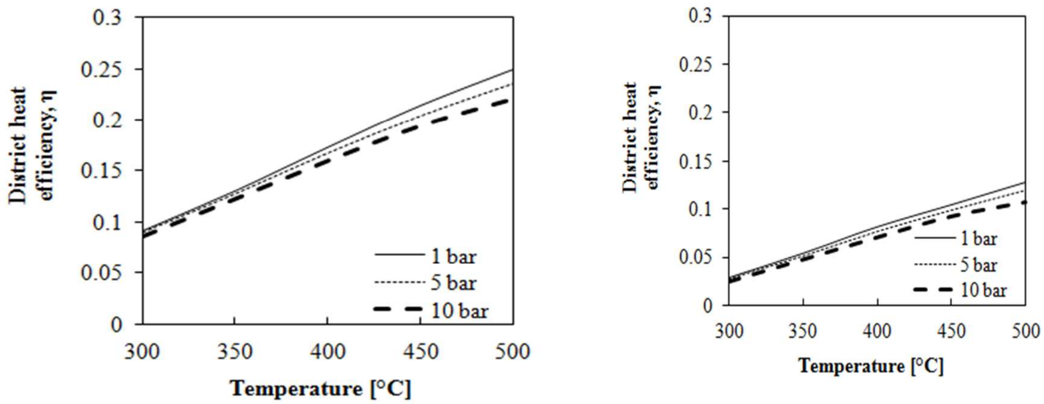

(a) (b)

This is the post-print version.
Published version dx.doi.org/10.1021/acs.energyfuels.6b03441

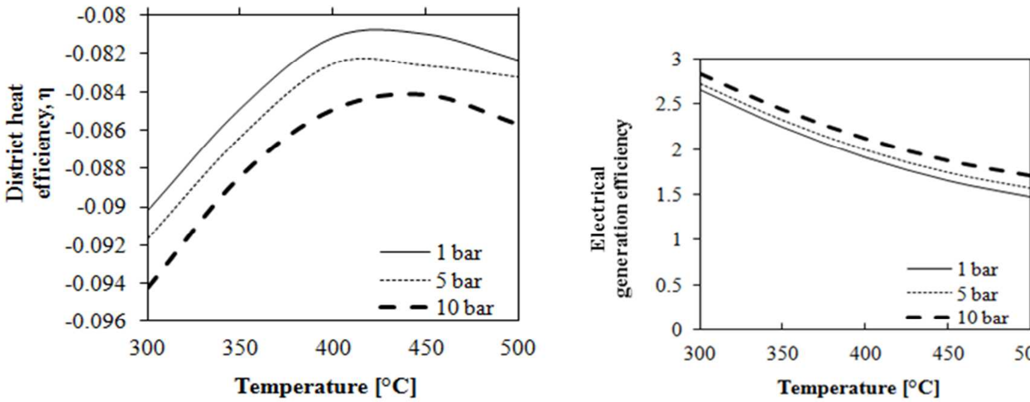

(c) (d)

Figure 9. Effect of moisture content (wet basis) on dictrict heat efficiency (a) 20%, (b) 40%, (c) 60% and electricity generation efficiency (d)

(a) (b)

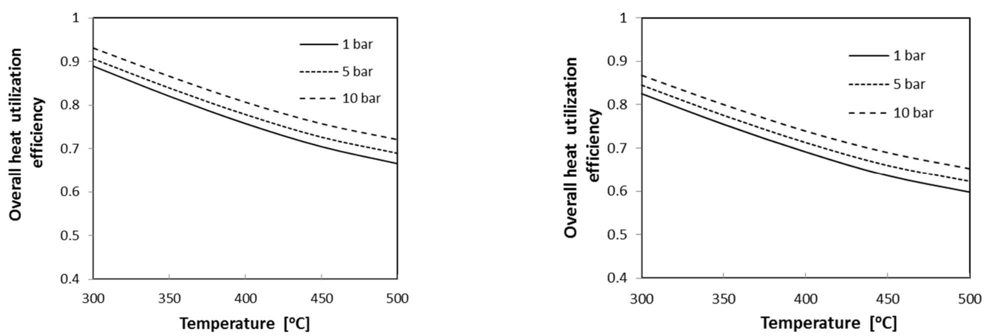

(c)

This is the post-print version.
Published version dx.doi.org/10.1021/acs.energyfuels.6b03441

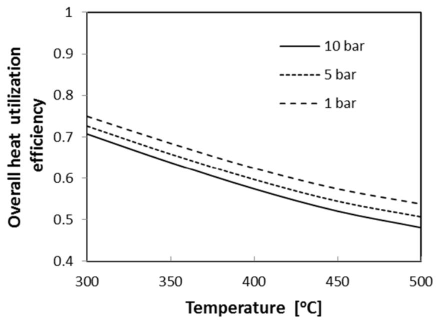

985 **Figure 10.** Overall heat utilization efficiency: (a) moisture content 20% wet basis, (b) 40%,

986 (c) 60%

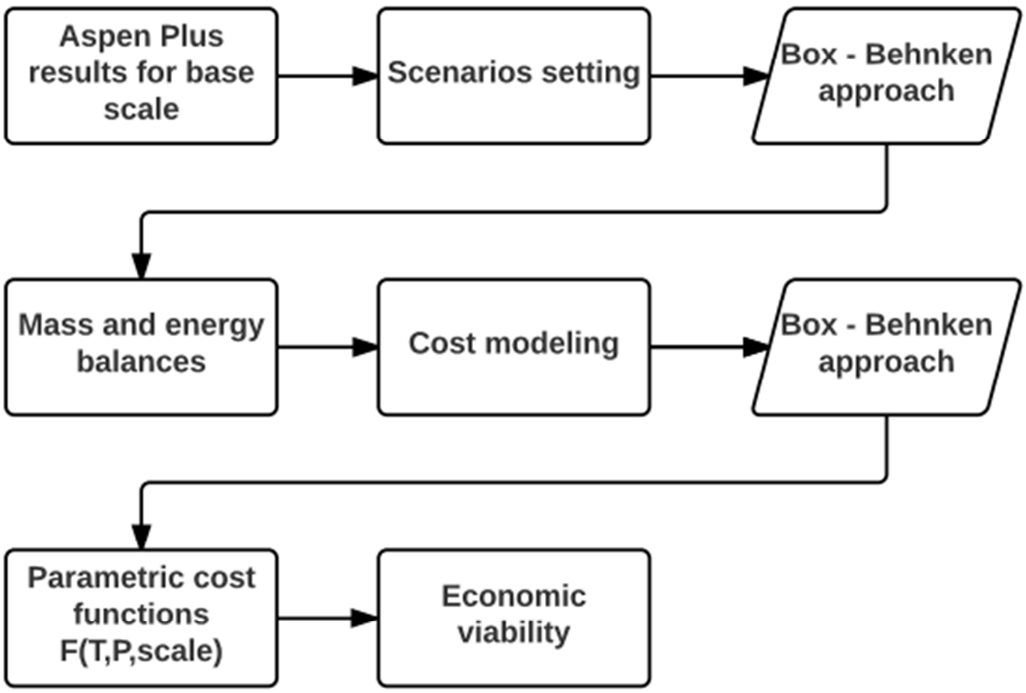

987

988 **Figure 11.** The workflow of techno – economic analysis

989

This is the post-print version.
Published version dx.doi.org/10.1021/acs.energyfuels.6b03441

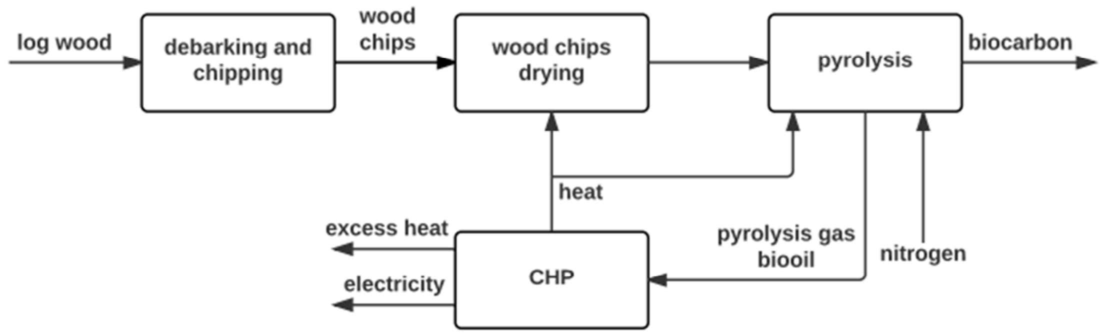

Figure 12. Simplified process flow diagram for Scenario A

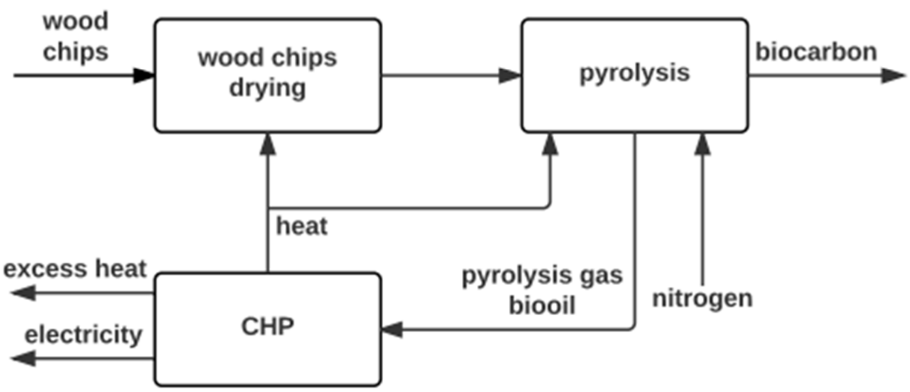

Figure 13. Simplified process flow diagram for Scenario B

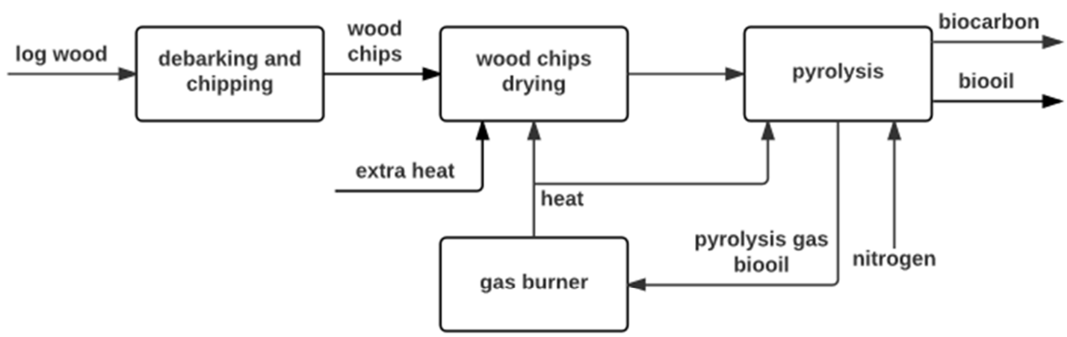

Figure 14. Simplified process flow diagram for Scenario C

This is the post-print version.
Published version dx.doi.org/10.1021/acs.energyfuels.6b03441

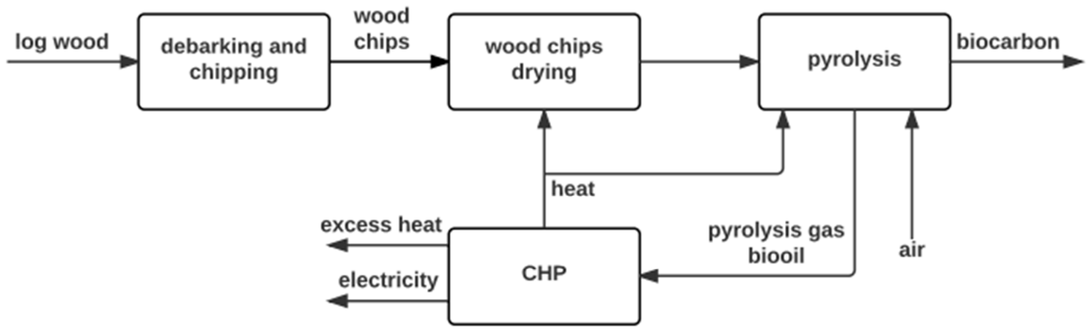

Figure 15. Simplified process flow diagram for Scenario D

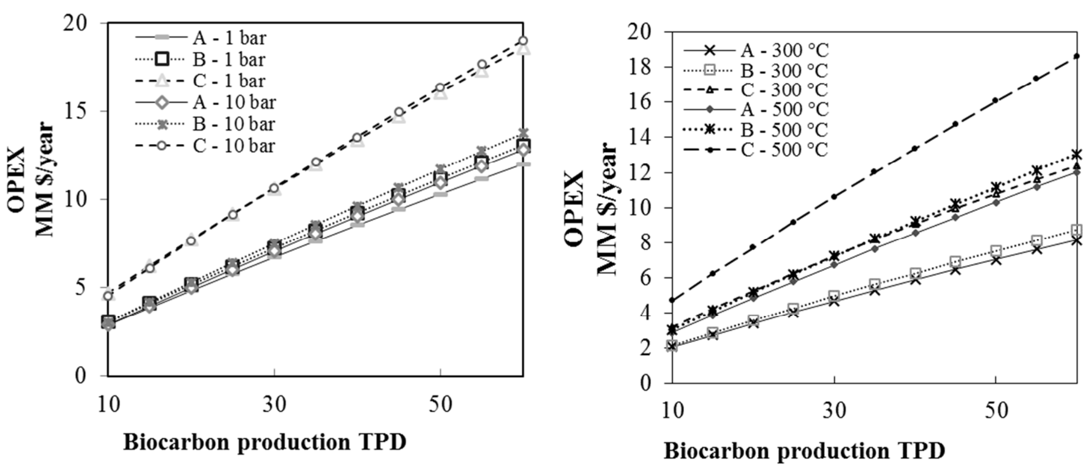

Figure 16. Influence of carbonization pressure (a) and temperature (b) on the OPEX for scenario A, B and C

This is the post-print version.
Published version dx.doi.org/10.1021/acs.energyfuels.6b03441

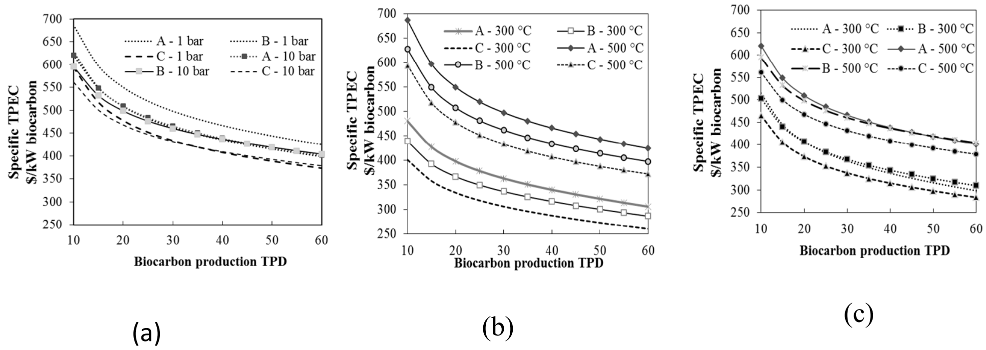

Figure 17. Influence of carbonization pressure (a) and temperature (b)-1 bar and (c)-10 bar on specific total purchase equipment cost (TPEC) for scenario A, B and C

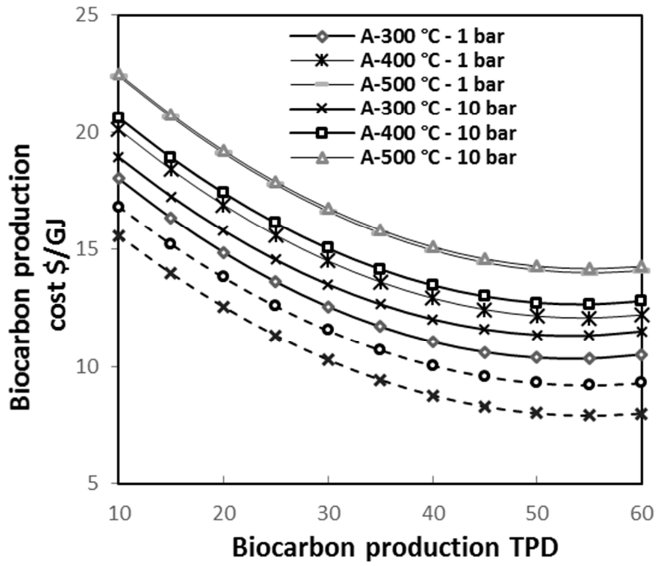

Figure 18. Influence of carbonization pressure and temperature for scenario A logwood conversion to biocarbon and Scenario C logwood conversion to biocarbon and biooil

This is the post-print version.
Published version dx.doi.org/10.1021/acs.energyfuels.6b03441

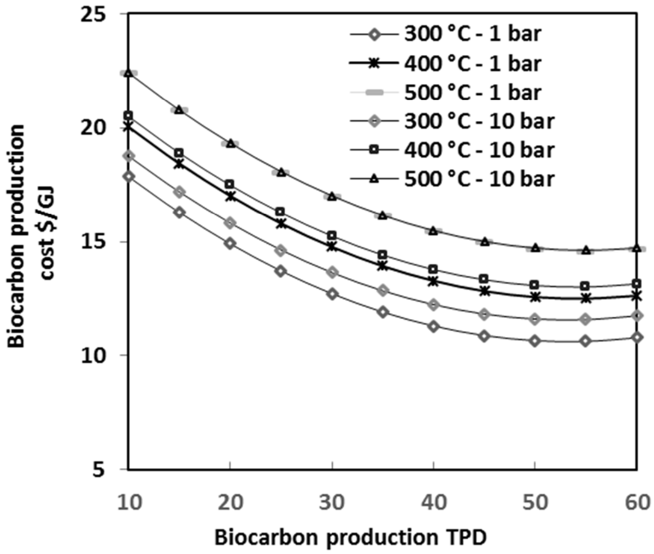

1018

1019 **Figure 19.** Influence of carbonization pressure and temperature for scenario B woodchips
1020 conversion to biocarbon

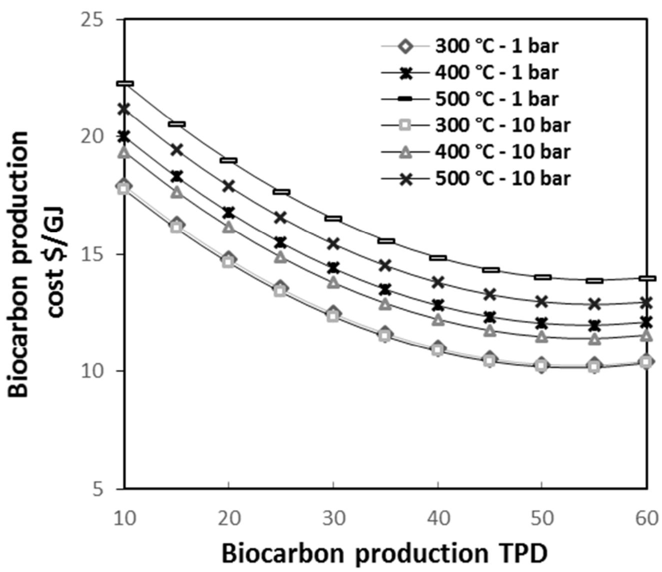

1021

1022 **Figure 20.** Influence of replacing inert agent from nitrogen to air for scenario D for
1023 logwood conversion to biocarbon

1024

1025

1026

1027

This is the post-print version.
Published version dx.doi.org/10.1021/acs.energyfuels.6b03441

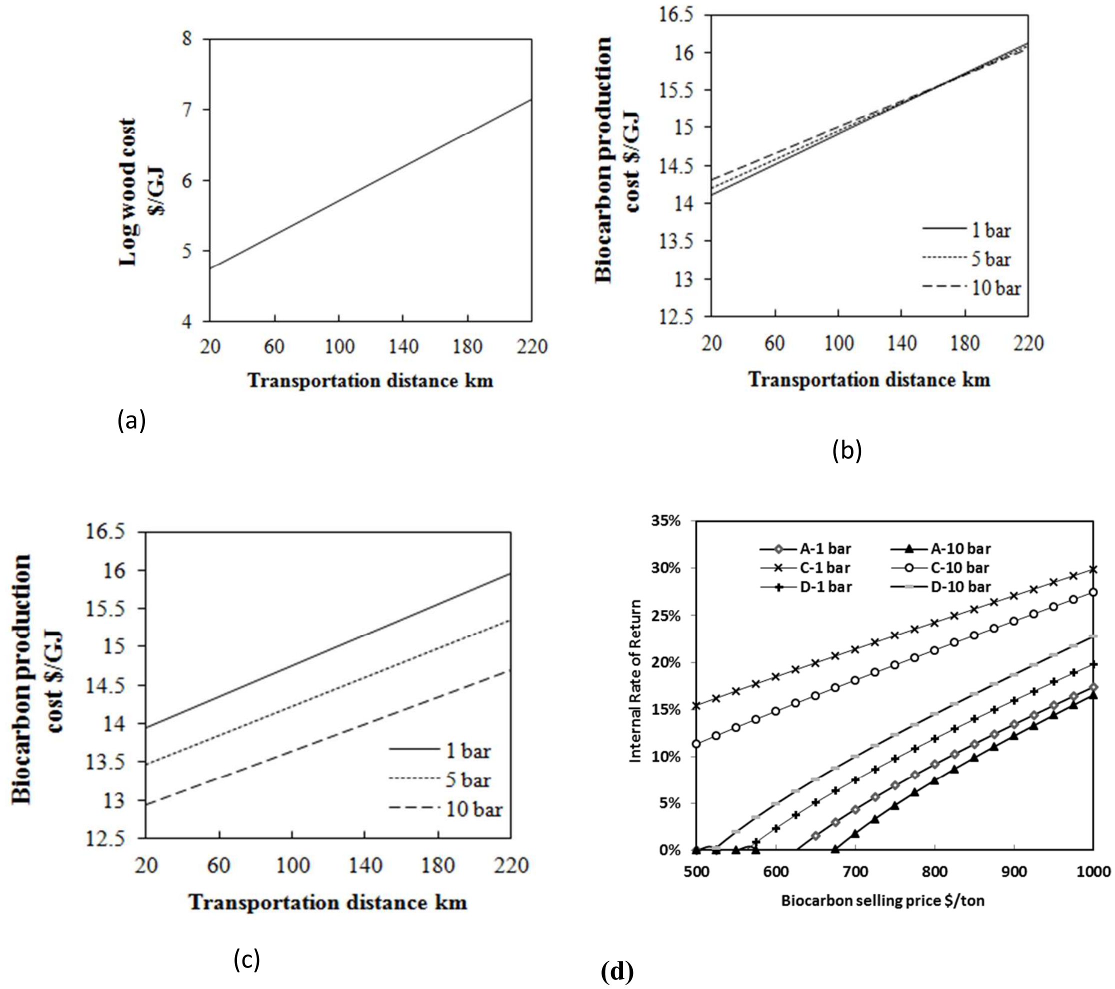

Figure 21. Influence of biomass transportation distance on (a) logwood cost, (b) biocarbon production cost for case A – nitrogen as pressurized gas, (c) biocarbon production cost for case D – air as pressurized gas and (d) internal rate of return versus biocarbon selling price for case A, C and D

Published version dx.doi.org/10.1021/acs.energyfuels.6b03441

1039

1040 List of Tables

1041 **Table 1.** Feedstock characteristics (Proximate and ultimate analysis, heating value)

Input fuel	Spruce stem wood	Spruce wood chips	Spruce bark	Spruce forest residues
Fixed carbon (% wt. dry)	27.27	19.65	26.85	24.49
Volatiles (% wt. dry)	72.43	79.97	70.62	69.82
Ash (% wt. dry)	0.30	0.38	2.53	5.69
C (% wt. dry ash free)	47.38	48.78	49.09	51.53
H (% wt. dry ash free)	6.40	6.27	6.06	6.51
O (% wt. dry ash free)	46.1	44.8	44.4	41.5
N (% wt. dry ash free)	0.09	0.13	0.45	0.44
S (% wt. dry ash free)	0.01	0.01	0.02	0.02
Cl (% wt. dry ash free)	0.002	-	0.04	0.02
HHV (MJ/kg dry)	19.90	20.13	20.25	19.94

1042

1043 **Table 2.** Woodchips size distribution

Size distribution (mm)	Weight fraction
63 – 45	0.04
45 – 31.5	0.08
31.5 – 16	0.69
16 – 8	0.06
8 – 3.15	0.09
3.15 – 0	0.03

1044

1045

1046

1047

1048

1049

1050

1051

This is the post-print version.
Published version dx.doi.org/10.1021/acs.energyfuels.6b03441

Table 3. Mass balance distribution (kg/kg dry ash free biomass) for 500 °C at different pressures

	Pressure [bar]					
	1	4	8	12	16	20
CHAR	0.30968	0.32469	0.34525	0.36642	0.38820	0.41059
BIOOIL(tar + water)	0.58667	0.57541	0.56000	0.54413	0.52780	0.51101
Tar	0.36039	0.34069	0.31372	0.28594	0.25735	0.22797
Phenol	0.18020	0.17035	0.15686	0.14297	0.12868	0.11398
Acetic acid	0.18020	0.17035	0.15686	0.14297	0.12868	0.11398
Water	0.22627	0.23472	0.24629	0.25819	0.27045	0.28305
GAS	0.11028	0.10647	0.10124	0.09586	0.09033	0.08463
H_2	0.00036	0.00036	0.00036	0.00036	0.00036	0.00036
CH_4	0.00727	0.00727	0.00727	0.00727	0.00727	0.00727
C_2H_4	0.00001	0.00001	0.00001	0.00001	0.00001	0.00001
CO	0.05131	0.05131	0.05131	0.05131	0.05131	0.05131
CO_2	0.05133	0.04752	0.04229	0.03691	0.03138	0.02568
TOTAL (CHAR+BIOOIL+GAS)	1.00663	1.00657	1.00649	1.00641	1.00632	1.00624

Table 4. Specification of process design parameters used in the analysis

Process parameter	Value
Biocarbon output	10 ton/day
Raw logwood moisture (wet state)	20 – 60%
Bark content (weight fraction)	8%
Air temperature to the dryer	170 °C
Air pressure to the dryer	2 bar
Chips moisture content after dryer (wet state)	10%
Pyrolysis temperature	300 – 500 °C
Pyrolysis pressure	1 – 10 bar
SH steam temperature	550 °C
SH steam pressure	60 bar
IP steam temperature	550 °C
IP steam pressure	20 bar
LP steam temperature	220 °C
LP steam pressure	4 bar
Condensate temperature	80 °C
Feed water temperature after economizer	145 °C
Flue gas to stack temperature	120 °C

This is the post-print version.
Published version dx.doi.org/10.1021/acs.energyfuels.6b03441

Table 5. Overview of the different scenarios

Scenario	Feedstock	Pressurized gas	Electricity production	Products	
A	Logwood	Nitrogen	Yes	Biocarbon	-
B	Woodchips	Nitrogen	Yes	Biocarbon	-
C	Logwood	Nitrogen	No	Biocarbon	Biooil
D	Logwood	Air	Yes	Biocarbon	-

Published version dx.doi.org/10.1021/acs.energyfuels.6b03441

Table 6. Biocarbon process equipments for the base scale scenario A (10 ton/day, 500 °C, 10 bar)

Equipment	Scale specification	Base scale S_b	Actual scale S	Max load/ train	C_{S_b,I_b} MM$	I/I_b	g	$f_{overall}$	$TPEC_i$ MM$	$C_{S,I,i}$ MM$	Ref
Logwood Storage	Mass, ton	33.5	2.26	110	1.000	1.457	0.6	2.34	0.174	0.591	[40]
Debarking And Chipping With Auxiliary Equipment	Mass flow rate, ton/day	36.0	2.08	85	1.008	1.457	0.6	2.34	0.182	0.621	[40]
DRYER - 3 Stages Belt	surface area, m^2	-	-	-	-	1.457	-	2.56	0.604	2.250	[41]
Dry Woodchips Storage	Mass flow rate, ton/day	33.5	1.33	110	1.000	1.457	0.6	2.34	0.123	0.418	[40]
Chips Conveyor	Mass flow rate, ton/day	33.5	1.33	110	0.350	1.457	0.8	2.37	0.027	0.091	[40]
Pyrolysis Reactor	Weight of the vessel, kg	-	-	-	-	1.946	-	4.14	0.452	3.642	[38]
Compressor	Power, MW	10	0.015	-	6.030	1.457	0.6	2.51	0.076	0.278	[40]
Biocarbon Conveyor	Mass flow rate, ton/day	33.5	0.42	110	0.350	1.457	0.8	2.37	0.010	0.036	[40]
Biocarbon Storage	Mass, ton	33.5	0.42	110	1.000	1.457	0.6	2.34	0.058	0.197	[40]
Steam Turbine And Steam System	MWe	10.3	0.13	-	5.100	1.457	0.7	2.37	0.236	0.815	[40]
Burner	Volumetric flow rate m^3/h	1.0	831.42	-	0.002	1.457	0.7	2.19	0.214	0.682	[37]
Flue Gas Scrubber	Volumetric flow rate m^3/s	10	1.94	64	0.053	1.457	0.5	2.50	0.023	0.085	[37]
Bag Filter	Volumetric flow rate m^3/s	1	1.94	-	0.005	1.474	1	2.50	0.009	0.034	[37]
								Total	2.188	9.741	

This is the post-print version.
Published version dx.doi.org/10.1021/acs.energyfuels.6b03441

Table 7. Purchase equipment cost (TPEC, MM$) for the different scenarios (10 ton/day, 500 °C, 10 bar)

Equipment Name	Scenario A	Scenario B	Scenario C	Scenario D
Feedstock Storage	0.174	0.160	0.174	0.174
Debarking And Chipping With Auxiliary Equipment	0.182	0.000	0.182	0.182
Dryer - 3 Stages Belt	0.604	0.604	0.604	0.604
Dry Woodchips Storage	0.123	0.123	0.123	0.123
Chips Conveyor	0.027	0.027	0.027	0.027
Pyrolysis Reactor	0.452	0.452	0.452	0.452
Nitrogen Compressor	0.076	0.076	0.076	
Air compressor				0.070
Biocarbon Conveyor	0.010	0.010	0.010	0.010
Biocarbon Storage	0.058	0.058	0.058	0.058
Steam Turbine And Steam System	0.236	0.236	0.000	0.236
Burner	0.214	0.214	0.137	0.214
Flue Gas Scrubber	0.023	0.023	0.017	0.023
Bag Filter	0.009	0.009	0.005	0.009
Total Purchase Equipment Cost (TPEC)	2.188	1.992	1.865	2.188
Total Purchase and Installation Cost	9.741	9.073	8.639	9.741
Total Permanent Investment (TPI)	13.424	12.504	11.906	13.424

This is the post-print version.
Published version dx.doi.org/10.1021/acs.energyfuels.6b03441

1118
1119
1120
1121
1122
1123
1124 **Table 8.** Cost associated factors to estimate the Total Permanent Investment (TPI) [33]

Factor	Cost associated factors	Typical value	Adopted value
f_{site}	Site preparation	0.05 – 0.2	0.05
$f_{building}$	Buildings	0.05 – 0.1	0.05
f_{land}	Land	0.05 – 0.1	0.05
f_{cont}	Cost of contingency	0.05 – 0.15	0.05
f_{eng}	Engineering	0.02 – 0.05	0.02
f_{dev}	Project development and	0.02 – 0.03	0.02
f_{com}	Commissioning	0.1	0.1

1125

1126

1127 Table 9. Labor cost for base scale plant of 10 ton/day biocarbon production

Position	Employed people, $E_{ppl,i}$	Salary $/year, D_i	Scaling factor, b_i
Plant Manager	1	120000	0
Plant Engineer	1	96000	0.6
Maintenance Support	1	72000	0.6
Lab Manager	1	72000	0
Shift Supervisor	1	72000	0.6
Lab Technician	1	72000	0.6
Maintenance Tech	1	72000	0.6
Shift Operators	4	72000	0.6
Yard Employees	1	60000	0.6
Clerks & Secretaries	1	72000	0.2
Total labor cost		$996 000	

1128

1129

1130

1131 **Table 10.** Indirect operational costs $C_{op,i}$

Indirect (Fixed) Operational Cost	Reference value
Maintenance, C_{maint}	2% C_{TPI}
Administration, C_{adm}	2% C_{TPI}
Insurance, C_{insur}	1% C_{TPI}

1132

1133

1134

This is the post-print version.
Published version dx.doi.org/10.1021/acs.energyfuels.6b03441

Table 11. Annual OPEX for different scenarios (10 ton/day, 500 °C, 10 bar)

Parameter	Scenario A	Scenario B	Scenario C	Scenario D
Biomass Supply	926 558	1 099 583	926 558	926 558
Fresh Water	593	593	432	593
Waste Water Treatment	10 159	10 159	7 411	10 159
Fly Ash Disposal	495	495	261	495
Nitrogen	333 793	333 793	333 793	-
Electricity	-	-	46 923	-
Heat	-	-	248 273	-
Labor cost	996 000	996 000	996 000	996 000
Maintenance	268 479	250 079	238 128	268 468
Administration	268 479	250 079	238 128	268 468
Insurance	134 240	125 039	119 064	134 234
Total, \$/year	2 938 796	3 065 819	3 154 971	2 604 974

Table 12. Biomass supply variables under Norwegian conditions

Parameter	Value
Biomass density	500 kg/m^3
Forest exploitation cost	200 NOK/m^3
Cost of chipping (if buying chips)	48.4 NOK/m^3
Fixed transport cost	24 NOK/m^3
Variable transport cost	0.6 NOK/m^3/km
Annual biomass production	1000 ton/km^2
1 NOK in USD	0.12 USD/NOK

Table 13. Coefficients for biomass cost supply calculation

Coefficient	A – logwood	B – woodchips
x_0	-325331	-400648
x_T	657	847
x_P	777531	913153
x_W	-4992	-4987
x_{TT}	0.34	0.35
x_{PP}	31453	36902
x_{WW}	34.1	33.4
x_{TP}	-2015	-2369
x_{TW}	223.74	262.85
x_{PW}	-10206	-11984

This is the post-print version.
Published version dx.doi.org/10.1021/acs.energyfuels.6b03441

Table 14. Financial parameters for biocarbon plant construction

Financial parameter	Values/assumptions
Debt equity ratio	70-30
Depreciation model	Straight line depreciation model, depreciation period 20 years
Construction and commissioning duration	3 years period
% required capital during construction and commissioning	30% year 1, 40% year 2 and 30% year 3
Income tax rate	28%
Loan repayment period	10 years
Interest rate	7%
Currency and reference year	US$ (2015)
Plant cost update	CEPCI 2015

Table 15. Direct variable operational costs and reference values for operational income [33]

Parameter	Value
Fresh water	0.4865 $/m^3$
Waste water	8.34 $/m^3$
Fly Ash disposal	40 $/ton
Nitrogen	0.353 $/Nm^3$
Electricity (scenario C)	0.111 $/kWh
Heat (scenario C)	70 $/MWh
Heat price	70 $/MW
Electricity price	0.111 $/kWh
CO_2 intensity (Norway crude oil)	6.2 gCO_2/MJ
CO_2 avoided emission	70 $/ton
Biooil price	500 $/ton

This is the post-print version.
Published version dx.doi.org/10.1021/acs.energyfuels.6b03441